Ecological Modelling 481 (2023) 110369

Contents lists available at ScienceDirect

Ecological Modelling

journal homepage: www.elsevier.com/locate/ecolmodel

A spatially explicit model of tree leaf litter accumulation in fire maintained longleaf pine forests of the southeastern US

Nuria Sánchez-López [a,*], Andrew T. Hudak [b], Luigi Boschetti [a], Carlos A. Silva [c], Kevin Robertson [d], E Louise Loudermilk [e], Benjamin C. Bright [b], Mac A. Callaham Jr. [e], Melanie K. Taylor [e]

[a] University of Idaho, Department of Forest, Rangeland and Fire Sciences, College of Natural Resources, 875 Perimeter Drive, Moscow, ID 83844, United States of America
[b] USDA Forest Service, Rocky Mountain Research Station, Forestry Sciences Laboratory, 1221 S Main Street, Moscow, ID 83843, United States of America
[c] Forest Biometrics, Remote Sensing and Artificial Intelligence Laboratory (Silva Lab), School of Forest, Fisheries, and Geomatics Sciences, University of Florida, Gainesville, FL 32611, United States of America
[d] Tall Timbers Research Station & Land Conservancy, 13093 Henry Beadel Drive, Tallahassee, FL 32312, United States of America
[e] USDA Forest Service, Southern Research Station, Center for Forest Disturbance Science, 320 Green St, Athens, GA, 30602, United States of America

ARTICLE INFO

Keywords:
Litter production
Litter accumulation
Surface fuels
Time since fire
Tree crown
Airborne laser scanning (ALS)

ABSTRACT

The continuity and depth of litter fuelbeds are major drivers of fire spread and fuel consumption. However, no established approach is available for the spatially explicit prediction of litter loads over large areas. Local fuel heterogeneity introduces large uncertainties on estimates derived from field-based models based on the extrapolation of sparse data samples. In fire-maintained pine forests of the southeastern US, litter accumulation and its distribution over the forest floor are mainly driven by vegetation productivity and by the number of years since the last fire (YSF). Some ecological models that simulate fire effects allow for a time-dependent estimation of litter by accounting for the opposing rates of litter deposition and decomposition as a function of YSF at the landscape level, but they do not account for spatial heterogeneity. We developed a conceptually simple approach for wall-to-wall estimation of tree leaf litter loads at high spatial resolution (5 m). The approach involved, first, estimating spatial patterns of tree annual litterfall. We mapped individual tree crowns through segmentation of airborne laser scanning (ALS) data, and we estimated crown foliage biomass using tree inventory data and ALS derived tree crown attributes. Tree annual litterfall was calculated as a fraction of the crown foliage biomass based on leaf turnover rates. We then quantified tree leaf litter accumulation through a spatially explicit implementation of the established Olson (1963) accumulation and negative decay model. We tested and validated our model in several management and research units at Eglin Air Force Base (Florida), Pebble Hill Plantation (Georgia), and Osceola National Forest (Florida), where managers maintain predominantly longleaf pine forests using frequent fire. Pixel-level RMSD and BIAS between tree leaf litter biomass estimated by the proposed model and reference field measurements were 0.21 and 0.01 kg m^{-2}, and area-level RMSD and BIAS were 0.09 and 0.01 kg m^{-2}. We concluded that linking patterns of litterfall and tree leaf litter accumulation to tree crown objects provides a means to characterizing the discontinuity of the litter layer, accounting for spatial heterogeneity largely traceable to tree crown foliage inputs.

1. Introduction

The continuity and depth of the surface vegetation and fuel layers are major drivers of fire spread and fuel consumption in frequently burned ecosystems and are linked to fire risk and severity (Agee and Skinner, 2005; Hiers et al., 2009; Loudermilk et al., 2012). High-resolution maps of these fuels are particularly relevant for predicting fire intensity and burn patterns in fire-maintained longleaf pine (*Pinus palustris*) forests of the North American Coastal Plain in the southeastern US (Noss et al., 2015). These systems are dependent on frequent (1–3 year interval) surface fires of low severity to maintain their high levels of plant diversity (Bond et al., 2005; Kirkman et al., 2001; Mitchell et al., 2009;

* Corresponding author.
E-mail address: nsanchezlopez@uidaho.edu (N. Sánchez-López).

https://doi.org/10.1016/j.ecolmodel.2023.110369
Received 10 November 2022; Received in revised form 8 March 2023; Accepted 21 March 2023
Available online 6 April 2023

Walker and Peet, 1984). Because of frequent fire, vegetation communities are characterized by widely spaced pine trees, resprouting hardwoods, and a continuous herbaceous layer mostly composed of perennials. The spatial arrangement of these communities defines the distribution and composition of the fine surface fuels, which are often dominated by tree leaf litter and particularly pine needle cast. These are the major contributors to fine surface fuel loading, often representing more than half of the available fine fuel (Jevon et al., 2022; Mitchell et al., 1999; Platt et al., 2016; Robertson et al., 2014; Thaxton and Platt, 2006). Consequently, tree litter is unevenly distributed over the forest floor depending on tree density and distribution (Grace and Platt, 1995). For instance, unburned patches are often observed to correspond to tree gaps and areas of low canopy cover, even when there is continuous herbaceous cover on the ground (Mugnani et al., 2019; Robertson et al., 2019).

Various methods, including analytical modeling, classifications, and/or statistical analysis using both field and remote sensing datasets have been proposed to quantify litter loads (Bright et al., 2022; Hudak et al., 2016; Keane, 2012; Keane et al., 2001; Loudermilk et al., 2011; Lydersen et al., 2015; Olson, 1963). For instance, Loudermilk et al. (2011) utilized field data and linear models to estimate pine and hardwood leaf litter loads as a function of time since fire and simulated tree size and spatial distribution. Hudak et al. (2016) used ALS and Landsat optical data to map forest structure and composition through imputation and reported functional relationships between overstory structure and surface fuel attributes. Bright et al. (2022) predicted surface fuels using remotely sensed data and several ancillary datasets, including topographic and fire history variables, on a study area across the Kaibab plateau in Northern Arizona. Nevertheless, the spatially explicit characterization of litter loads is still a challenge over areas larger than field sample plots. Local fuel heterogeneity introduces large uncertainties in estimates and interpolations derived from field data, and its systematic monitoring is time-consuming and expensive, requiring intensive sampling protocols and frequently repeated measurements (Keane, 2015; Keane et al., 2001). Additionally, the usefulness of remote sensing for direct modeling and mapping of such fine fuels is limited due to the low sensitivity to litter depth of both active and passive sensors, which is further limited under the forest canopy.

Leaf litter generally accumulates over time until litter production is balanced by decomposition in a quasi-equilibrium (McCaw et al., 2002; Olson, 1963; Zazali et al., 2020). Litter production (or litterfall) results from senescent biomass irregularly falling to the forest floor from all layers of the vegetation canopy, a process mainly driven by aboveground biomass, species characteristics, and climate (Costa et al., 2020; Keane, 2008; Neumann et al., 2018). Decomposition, which drives the rate of nutrient recycling in the forest ecosystem, is controlled by heterotrophic consumption of organic composites and in turn depends on litter quality, soil properties, and climatic factors (Bezkorovaynaya, 2005; Keane, 2008; Krishna and Mohan, 2017; Prescott, 2002). A widely used litter accumulation model that combines two simple analytical models for litter deposition and decomposition was introduced by Olson (1963). The model assumes that litter falls at a constant rate and that at each point in time decomposition is proportional to the total litter accumulation. The combination of these two terms results in a negative exponential model, where total litter accumulation is a function of the time since the litter deposition was initiated, such as following planting, or a fire that fully or mostly consumed the litter. While the Olson model ignores factors such as tree size and distribution, stand age, productivity, and annual and seasonal variations in precipitation and temperature to describe the spatial intra-stand heterogeneity of the litter loads, it has been widely used by fire ecologists as it provides realistic litter accumulation estimates (Zazali et al., 2020).

Assuming relatively similar soil and climate conditions, spatial variability in litter accumulation would be primarily driven by canopy characteristics. Canopy structure and aboveground biomass affects the spatial variation of surface litter by both influencing the organic layer environment (e.g., soil temperature, water content) of microbes that drive decomposition and by governing the litterfall (Hopkins et al., 2020; Neumann et al., 2018; Penne et al., 2010; Platt et al., 2016). Therefore, characterizing the spatial variability of foliage biomass driven by heterogeneity in the forest canopy provides a means to describe patterns of litterfall and surface fuel dynamics at the scale of tree crowns (Ferrari and Sugita, 1996; Yarie, 2000).

Remote sensing currently provides the most practical means to characterize patterns of aboveground biomass across forested landscapes and associated ecosystem processes. Airborne laser scanning (ALS) shows particular promise because of its ability to record a dense 3D point cloud that can be used to characterize the forest canopy structure. ALS has been successfully used for tree detection, stem mapping, and segmentation of tree crowns (Jakubowski et al., 2013; Li et al., 2012; Roussel et al., 2020; Silva et al., 2016). ALS tree crown-derived metrics have been used to quantify tree attributes such as height, volume, and/or woody and foliar biomass using different modeling approaches including parametric and non-parametric methods (Chen et al., 2007; Rocha et al., 2023; Silva et al., 2016; Wan Mohd Jaafar et al., 2018).

The overarching objective of this study is to develop a conceptually simple and physically-based model of tree leaf litter accumulation after fire. The proposed model is informed by remote sensing data that capture the spatial heterogeneity of litter loads in temporally dynamic, fire-maintained longleaf pine forests. The methodology is demonstrated primarily at three study sites located in pine forests in the southeastern US, where field data, prescribed fire records, and ALS data were available for testing and validating the methodology (Section 2). The model estimates litter accumulated at the 5 m resolution in three main steps (Fig. 1). First, tree leaf litter production (i.e., tree annual leaf litterfall) is estimated at the scale of projected tree crowns (Section 3.1). This model is driven by tree crown attributes calculated from ALS data, and it is informed by tree inventory data, allometric equations, and species traits (e.g., leaf lifespan). Second, tree leaf litter accumulation since the last fire is estimated through a spatially explicit implementation of the Olson (1963) model that incorporates the outputs of the production model, a decomposition rate—estimated as a function of the annual actual evapotranspiration (AET) that accounts for temperature and moisture—, and fire history maps (Section 3.2). Finally, we evaluate the accuracy of the tree leaf litter accumulation model at a pixel and a multi-pixel level (i.e., area-level accuracy assessment) by leveraging independent litter biomass field measurements collected at the study sites (Section 3.3).

2. Materials

2.1. Study sites

The three study sites were Eglin Air Force Base (AFB) in the Florida Panhandle, Pebble Hill Plantation (PHP) in southern Georgia, and the Olustee Experimental Forest within the Osceola National Forest (ONF) in northeastern Florida (Fig. 2). The sites undergo frequent prescribed burning (often a 1–3 year fire return interval) that serves to maintain the native wildlife and health of the predominant longleaf pine ecosystem as well as facilitating military training at Eglin AFB. The three sites share the same subtropical climate with relatively mild winters and warm and humid summers, but they span the edaphic gradient characteristic of the region, described below.

Eglin AFB covers 186,350 ha and it is divided into management units where activities such as prescribed fires or silviculture practices are performed. The Eglin AFB portion of our study focuses on sandhill and flatwoods longleaf pine communities (FNAI, 2010) where ALS data were most recently collected in 2018 (~92,699 ha) (Fig. 2). The sandhill pine communities are located on soils in the Entisol order composed of deep sand (Soil Survey Staff, 2021). The vegetation is characterized by a discontinuous overstory of longleaf pine and some slash pine (*P. elliotti*)

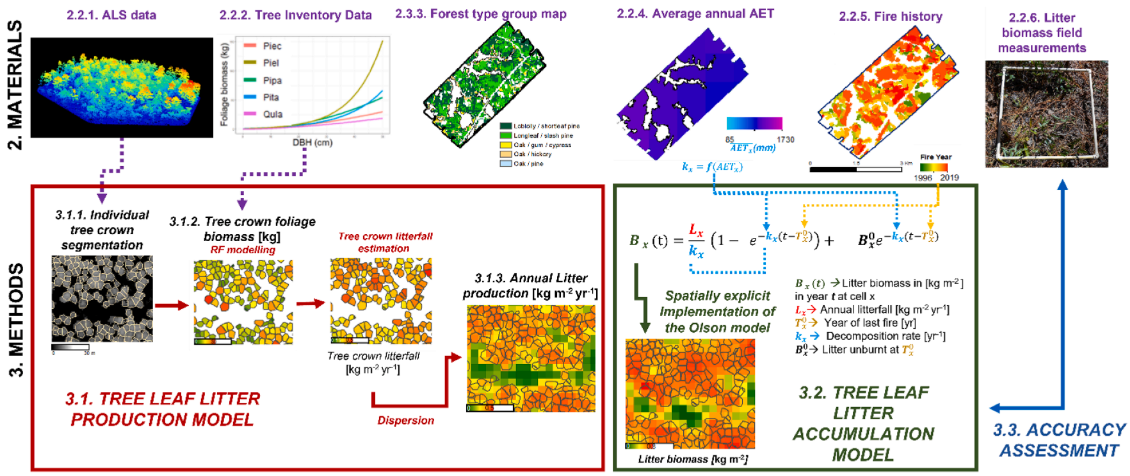

Fig. 1. Workflow of the spatially explicit model of litter accumulation based on a tree crown-level litter production model and a spatially explicit implementation of the Olson model. Headings refer to the material and method sections in the paper.

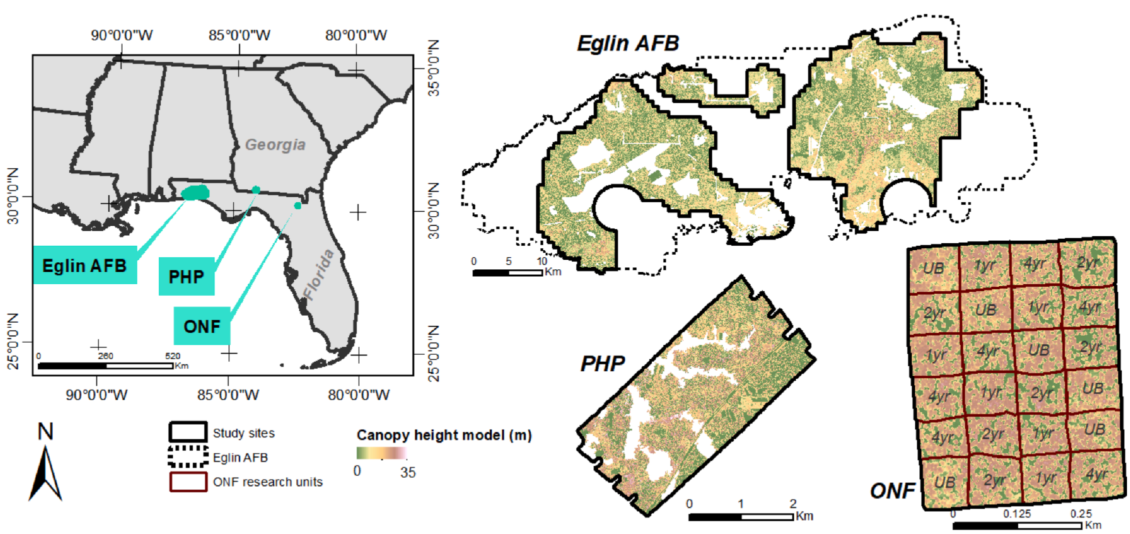

Fig. 2. Location of the study sites at Eglin Air Force Base (AFB), Pebble Hill Plantation (PHP), and Osceola National Forest (ONF). The canopy height model derived from airborne laser scanning (ALS) is displayed as background within the study sites. A mask of pine dominated forest stands was applied at Eglin AFB and PHP. UB: unburnt units at ONF (also labeled are units maintained at 1 yr, 2 yr, or 4 yr fire return intervals).

with a discontinuous midstory of fire-tolerant broadleaf species, mostly turkey oak (*Quercus laevis*) and bluejack oak (*Q. incana*), as well as less fire hardy broadleaf species such as persimmon (*Diospyros virginiana*). The surface vegetation is species-rich with forbs, perennial grasses dominated by wiregrass (*Aristida stricta* var. *beyrichiana*), and broadleaf woody plants that are topkilled by fire and resprout. The flatwoods communities are located on soils in the Spodosol order, where the deep sand soil is saturated for part of the year and contains some organic material (Soil Survey Staff, 2021). Flatwoods also have a discontinuous canopy of mostly longleaf pine and some slash pine, but with a midstory and understory of evergreen woody plants, mostly saw palmetto (*Serenoa repens*), dwarf live oak (*Q. minima*), and gallberry (*Ilex glabra*) (Hudak et al., 2016) that resprout after being topkilled, and forbs and perennial grasses dominated by wiregrass. At PHP, the study site covers 824 ha within upland longleaf pine communities (FNAI, 2010) located on soils in the Ultisol order, with sandy topsoil and a clay-rich sub-horizon (Soil Survey Staff 2021). The overstory vegetation is dominated by a mix of longleaf pine and shortleaf pine (*P. echinata*), while the understory is dominated by a particularly species-rich community of perennial grasses including wiregrass, forbs, and resprouting broadleaf woody plants (Ostertag and Robertson, 2007; Robertson and Hmielowski, 2014). Finally, the study site at ONF consists of winter experimental burn units within flatwoods pine communities as described above. The ONF site is part of a long-term fire experiment that was first established in 1958 in a randomized block design to evaluate different fire return intervals on fuel accumulation. It is comprised of six replicates of four treatments (~0.85 ha each) that consist of burns performed regularly every 1, 2, or 4 years, with an additional no-burn treatment (control) (McKee, 1982). Overstory and understory vegetation are dominated by longleaf pine and saw palmetto, respectively.

All three sites represent native vegetation types where the soil has not been previously disturbed by agriculture or other management, and all three have been burned frequently for decades leading up to this study. Because of frequent fire, surface organic matter is dominated by litter in various stages of decomposition but with very little organic soil/duff (except in the ONF unburned control units). The three community types studied represent the three dominant soil orders and respective ecosystem types in the North American Coastal Plain (Carr et al., 2010) and thus provide broad representation of the region.

2.2. Data

2.2.1. Airborne laser scanning data

ALS data were used to segment individual tree crown maps within the study sites and to compute crown attributes that were used as predictors of foliage biomass in a random forest (RF) model (Section 3.1). ALS data were acquired in 2018 at both Eglin AFB and PHP, and between 2018 and 2020 at ONF. The average return density was variable among sites and campaigns but always exceeded 8 points m^{-2}. The point cloud (provided in a .laz or .las binary format) was normalized, converting points to height above ground using LAStools software (Isenburg, 2021). A canopy height model (CHM, 1 m spatial resolution) was created using the 'grid_canopy' function and the pit-free algorithm (Khosravipour et al., 2014) implemented in the 'lidR' R package (Roussel et al., 2020).

2.2.2. Tree inventory data

Tree inventory data provided the foliage biomass dataset used as the response variable to train the RF model (Section 3.1.2). Because of the limited number of inventory plots on the three study sites, the dataset was augmented with additional plots located in longleaf pine-dominated forests with similar environmental conditions, where contemporaneous ALS data were also available (Appendix A, Figure A1).

Within each inventory plot, tree species, health status (healthy, unhealthy, and dead), and dbh (diameter at breast height, 1.37 m) were recorded. Tree attributes such as stem geolocations, tree height, and crown diameter—calculated as the average of two measurements in orthogonal directions of the projection of the edges of the crown—were available for a subset of plots (19 plots encompassing a total of 615 trees). The data used for training the foliage biomass model were located at two of the primary study sites (Eglin AFB, PHP) and at three similar southern pine forest sites: Tall Timbers Research Station (TTRS, Florida), Ft Stewart (Georgia), and Ft Jackson (South Carolina) (Appendix A, Table A1). Supplementary tree inventory plot data missing the geolocation of the individual stems, tree height, or the crown diameter were used for assessing the accuracy of the mapped foliage biomass estimates; these plots were located at Eglin AFB, ONF, PHP, TTRS, Ft. Jackson, Ft. Stewart, and the Joseph Jones Ecological Research Center (JERC) (Appendix A, Table A2). A detailed description of the tree inventory datasets, tallied species, and collection protocols is provided in Appendix A (Section 1.2).

Only live trees with ≥10 cm dbh were considered. Tree foliage biomass was estimated by applying published species-based allometric equations (Gonzalez-Benecke et al., 2014, 2018 ; Loomis et al., 1966; Mitchell et al., 1999; Zhao et al., 2015, 2016, 2019a,b) (Appendix A, Section 2.1).

2.2.3. Forest type group map

The 30 m resolution Forest Type Groups of the Continental United States dataset (USDA-FIA, 2021) was used to parametrize wall-to-wall the leaf turnover rate (LTR) in the spatially explicit annual tree leaf litter production model (Section 3.1.3). The map is generated through the imputation of Forest Inventory and Analysis (FIA) field data collected from 2014 to 2018 to phenological variables derived from Landsat OLI (Operational Land Imager) satellite data, together with auxiliary climatic and topographic data (Wilson et al., 2012, 2013, 2018). The map defines a forest type group for every 30 m forested pixel, adopting the same legend (33 forest type groups) of the Forest Atlas of the United States (USDA-USFS, 2022). The longleaf/slash pine group is predominant in all three study sites, with a significant presence of the loblolly/shortleaf pine group at PHP (Fig. 3).

2.2.4. Average annual evapotranspiration

Actual evapotranspiration (AET) was used to estimate the litter decomposition rate, which is one of the parameters required by the litter accumulation model (Section 3.2). Annual AET from 2003 to 2019 was obtained from the Moderate Resolution Imaging Spectroradiometer (MODIS) product (1 km) available at https://earlywarning.usgs.gov (accessed on 9th of September 2021). This product uses the operational simplified surface energy balance (SSEBop) model to retrieve annual AET (Senay and Kagone, 2019; Senay et al., 2013). For the three sites, the annual average was computed (Fig. 4). Average annual AET was higher at ONF (1292 mm) and PHP (1055 mm) than at Eglin AFB (653 mm), as expected based on temperature and precipitation trends (Thornton et al., 2020).

2.2.5. Fire history

The fire history of the study sites was used to assess the time since fire and, therefore, the time of the litter accumulation process (Section 3.2). It was reconstructed by integrating management records and remotely sensed derived products (Fig. 5).

At Eglin AFB recurrent fire is used as a management tool to ensure appropriate conditions for military training and maintain the longleaf pine forest communities. Fire records at Eglin AFB consisted of geographic information system (GIS) datasets of fire boundaries, which included the date of burn from 1972 up to 2015.

At PHP, fires are typically applied to pine communities at 1–2 year intervals as part of the regional tradition for game management (Robertson and Hmielowski, 2014; Rother et al., 2020). The Southeast FireMap 'pilot' product of TTRS and USDA Natural Resources Conservation Services (NRCS) produced from Landsat satellite data was used as fire history at PHP (Southeast (SE) FireMap, 2021). This product maps detectable fires happening since 1994 (both managed prescribed burns and wildfires) across nine states in the southeastern US. Within the boundaries of the study site at PHP, reported fires span from 1996 to 2019.

At ONF, burns are regularly performed every 1, 2, or 4 years on the three burn treatment blocks, or are excluded on the no-burn treatment (control) blocks. Fig. 5 shows the fire history records available within

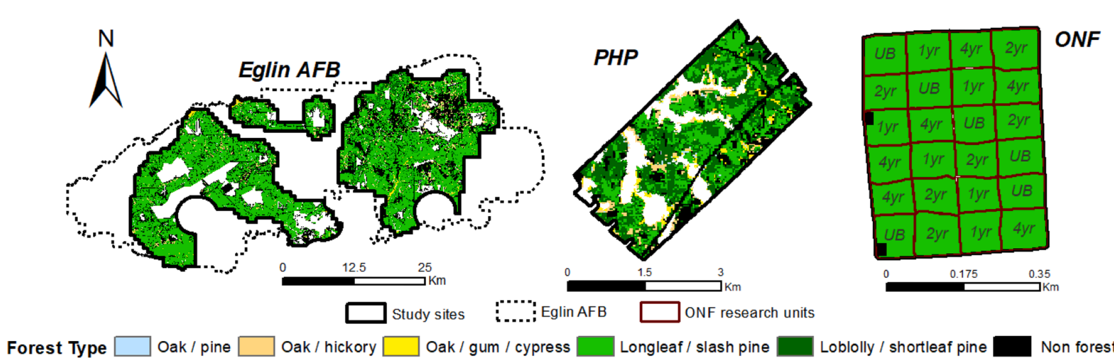

Fig. 3. Forest type groups at Eglin AFB (left), Pebble Hill Plantation (PHP) (middle), and Osceola National Forest (ONF) (right). UB: unburnt units at ONF (also labeled are units maintained at 1 yr, 2 yr, or 4 yr fire return intervals).

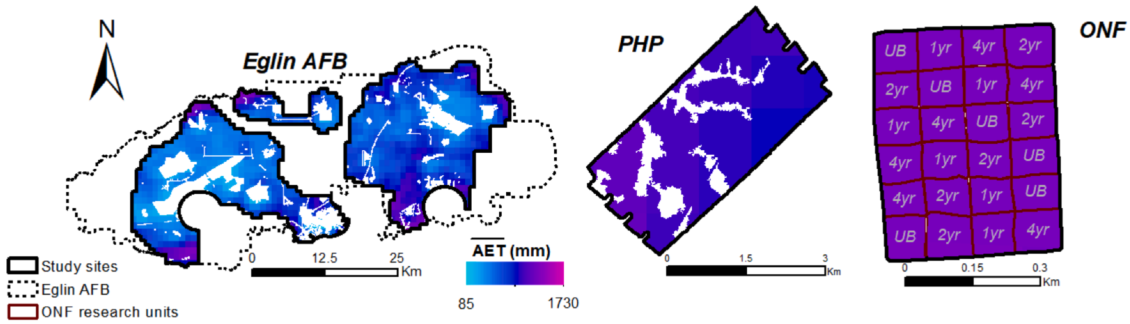

Fig. 4. Average annual actual evapotranspiration ($\overline{AET}$, mm) at Eglin AFB (left), Pebble Hill Plantation (PHP) (center), and Osceola National Forest (ONF) (right) obtained from the SSEBop Evapotranspiration MODIS derived product (Senay and Kagone, 2019). UB: unburnt units at ONF (also labeled are units maintained at 1 yr, 2 yr, or 4 yr fire return intervals).

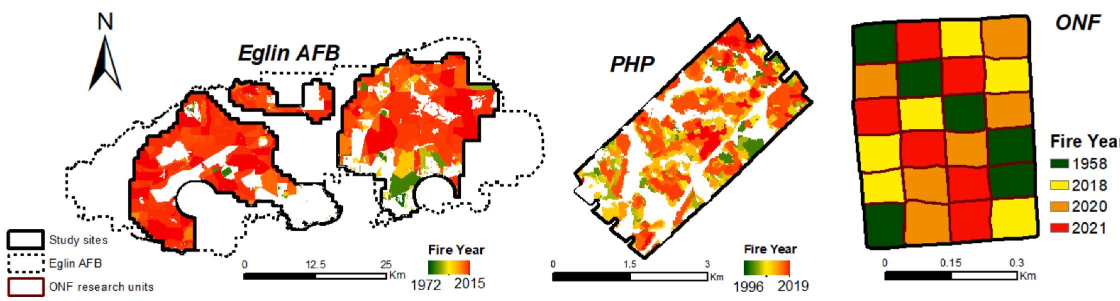

Fig. 5. Left, most recent fire between 1972 and 2015 at Eglin AFB, as reported in management records; center, most recent fire happening between 1994 and 2019 at PHP according to the SE FireMap; right, most recent fire (as of January 2022) at ONF experimental forest.

the three study sites up to 2015 for Eglin AFB, 2019 for PHP, and January 2022 for ONF.

2.2.6. Litter biomass field measurements

Previously collected litter biomass field measurements were collated and used for the accuracy assessment of the results of the proposed litter accumulation model at Eglin AFB and PHP, whereas new data were collected at ONF. These measurements consisted of destructive biomass sampling on square or circular plots (known as clip plots) in which biomass of different surface fuels (e.g., litter, shrubs, downed woody debris, grasses) was collected, bagged and oven-dried.

At Eglin AFB, three management units were sampled (i.e., 703C, 608A, and L2F), and surface fuel data were collected over 166 square clip plots in 2011 (1 m^2) and 2012 (0.25 m^2) in the framework of the RxCADRE (Prescribed Fire Combustion and Atmospheric Dynamics Research Experiment) project (Fig. 6) (Ottmar et al., 2015; Ottmar and Restaino, 2014). In 2011, 100 clip plots were established in five locations within the 703C and 608A units. In 2012, 66 samples were collected in the L2F unit; 36 were on three highly instrumented plots (HIPs) (west, east, and south HIPs), whereas the other 30 clip plots were systematically located along three parallel transects (Figs. 6 and 7) (Hudak et al., 2015; Hudak and Bright, 2014). All litter was collected, but it was not sorted, so the samples included pine needles, oak and broad leaves, and other tissue. Loads ranged from 0.05 to 1.27 kg m^{-2} (Table 1).

Another field campaign to characterize fuels was conducted at Eglin AFB in 2015 within the framework of a past SERDP (Strategic Environmental Research and Development Program) funded project. The sampling was stratified based on canopy height and percent canopy cover to represent the flatwoods and sandhills for open, single tree, and tree clump conditions. Twenty-four plots were established in five management units that burned 2 years before data collection (Fig. 6). Each

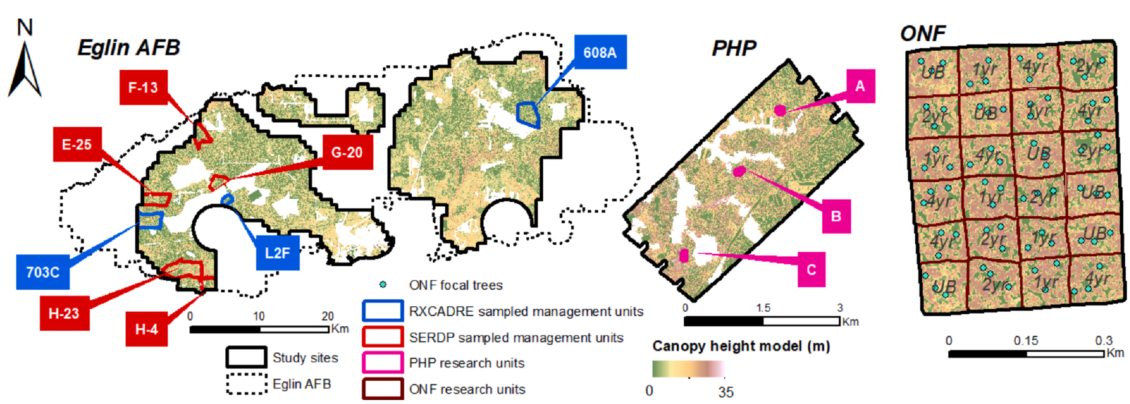

Fig. 6. Location of the 8 management units sampled in 2011, 2012 (RxCADRE), and 2015 (SERDP) at Eglin AFB; location of the 24 research units at the three locations (A, B, C) at Pebble Hill Plantation (PHP) where litter biomass was collected between 2006 and 2020; and location of the 72 randomly selected focal trees at Osceola National Forest (ONF) study site. UB: unburnt units at ONF (also labeled are units maintained at 1 yr, 2 yr, or 4 yr fire return intervals).

Table 1
Field clip plots measured at Eglin AFB, Pebble Hill Plantation (PHP), and Osceola National Forest (ONF) used for validation of model predictions. The table summarizes the number of clip plots, and minimum, maximum, mean, and standard deviation of the litter biomass (LB) (kg m^{-2}) for each site. Years since fire (YSF) indicates the number of growing seasons since the most recent previous prescribed fire. UB: unburnt (64 YSF). Std Dev.: standard deviation of LB measurements.

Study site	Accuracy assessment	Geolocation resolution	Units	Sampling year	YSF	Litter type	# Clip plots	Min. LB (kg m^{-2})	Max. LB (kg m^{-2})	Mean LB (kg m^{-2})	Std Dev. (kg m^{-2})
Eglin AFB RxCADRE	Pixel & area-level	Clip plot	703C, 608A	2011	2	All litter	100	0.05	0.75	0.33	0.16
			L2F	2012	3		66	0.00	1.27	0.48	0.31
Eglin AFB SERDP	Pixel-level	Clip plot	E-25, F-13, G-20, H-23, H-4	2015	2	Pine, oak, broad leaf	96	0.00	0.75	0.29	0.18
ONF	Pixel-level	Clip plot	All units	2022	1	Pine needle	216	0.07	0.50	0.26	0.09
					2		216	0.04	0.67	0.26	0.11
					4		216	0.13	0.83	0.42	0.14
					UB		216	0.11	1.08	0.47	0.19
PHP	Area-level	Research unit	A, B, C	2006–2020	1	Pine needle	300	0.00	0.55	0.12	0.09
					2		204	0.00	0.84	0.16	0.12
					3		155	0.01	0.90	0.20	0.16
					4		58	0.01	0.44	0.18	0.11
					5		36	0.00	0.54	0.18	0.16
					6		6	0.05	0.67	0.26	0.21

plot center was geolocated, and surface fuels were collected in four clip plots (0.25-0.50 m^2) located 5 m from the plot center in azimuthal directions 60°, 120°, 240°, and 300°, totaling 96 clip plot measurements. Different fuel categories were sorted including pine needles and fine litter, and oak and other broad leaves. Grass was not separated from pine litter during data collection, but an ocular estimation of the percentage of each component was noted when possible. Litter loads including pine and broad leaves ranged from 0.00 to 0.75 kg m^{-2} (Table 1).

At PHP, litter of pine needles was collected at 24 replicated research units (~0.12 ha) burned in May-June at 1–6 year intervals between 2006 and 2020. These units were in three localized sites (A, B, C) across the larger PHP property under study (Figs. 6 and 8). There were 4–6 collections per fire totaling 759 samples over the collection period. Clip plot geolocations were not recorded, and the number of measurements per years since fire (YSF) was lower for longer fire return intervals. Pine needle biomass ranged from 0.00 to 0.90 kg m^{-2} and was variable among sites (Table 1).

At ONF, litter was sampled in the 24 research units between January and February 2022 (Fig. 6). The sampling protocol was designed to address the non-random distribution of surface fuels expected on the forest floor based on canopy cover, i.e., considering the trees as the main source of litter inputs. Three focal trees per unit were randomly selected and geolocated using a Trimble Geo7x GPS (Fig. 6). Litter was collected within square clip plots (0.09 m^2) along transects leading away in the cardinal directions (N, S, E, W) from the base of the focal tree at 1, 2, and 4 m. The data were collected in all the units in the days immediately preceding the prescribed fires. YSF ranged from 1 to 4 years except for the unburned units that were 64 YSF, as the last burn was in 1958 (Table 1).

3. Methods

The workflow of the proposed model is presented in the conceptual diagram of Fig. 1. It involves three main steps. First, we map annual litter production using ALS data, tree inventory data, and ancillary data to estimate foliage biomass at the tree crown level and to inform litterfall patterns (Section 3.1). In the second step, we quantify tree leaf litter accumulation through a spatially explicit implementation of the Olson (1963) accumulation model (Section 3.2). We finally assess the accuracy of the model by comparing our estimates to independent litter biomass measurements from the field (Section 3.3).

3.1. Tree leaf litter production model

The spatially explicit estimation of litter production involves (1) generation of an individual tree crown map through segmentation of ALS data and computation of tree crown attributes from the ALS point clouds; (2) estimation of the total foliage biomass of each tree crown through RF modeling; and (3) estimation of annual litterfall at the crown level from leaf turnover rates and litter dispersal over the forest floor using a convolution filter.

3.1.1. Individual tree crown segmentation

The individual tree crown (ITC) segmentation was generated from the ALS data, using the R 'lidR' and 'lidRplugins' packages (Roussel et al., 2020). First, the locations of treetops were identified by applying the 'multichm' algorithm, based on iterative CHM generation from the point cloud, and a sequential detection of potential tree tops step using a local maximum filtering approach within a moving window over various CHMs (Eysn et al., 2015). The treetop locations and the CHM raster were subsequently used in the 'silva2016' segmentation algorithm (Silva et al., 2016) to generate the ITC segments. The parameters of both processing steps were set by the interpreter, assessing visually the accuracy of the segmentation (Appendix A, Section 2.3). The segmentation was performed on the full ALS extent of the three study sites (Fig. 2), and at additional sites at TTRS, Ft Stewart, Ft Jackson, and JERC where the tree inventory data were used for the accuracy assessment of the foliage biomass estimates (Appendix A, Figure A2).

For each ITC segment, 28 crown attributes were calculated from the ALS point cloud (Table 2) to be used as predictors in the RF foliage biomass model. None of the inventoried trees on the training plots (Appendix A, Table A1) and only four trees (<0.04% trees) on the assessment plots had an estimated crown projected area smaller than 1 m^2. Besides that, all trees were at least 10 cm of dbh. Therefore, segments with a crown area smaller than 1 m^2 or with crown height lower than 1.37 m, were removed from the segmentation. Crown height was defined by the 99th percentile of return height (Table 2).

3.1.2. Crown-level foliage biomass estimation

Tree crown foliage biomass (kg) was estimated for each ITC segment through RF modeling using the 'randomForest' package in R (Breiman, 2001; Liaw and Wiener, 2002; R Core Team, 2021). The methodology was adapted from Rocha et al. (2023), and the processing steps are summarized as follows. The detailed description is reported in Appendix A.

The RF was trained using as the response variable foliage biomass estimated through allometric equations for each measured tree included in the inventory dataset and using as predictor variables the crown attributes derived from the ALS data (Appendix A, Section 2.2). ITC segmentation was first performed on the ALS data covering each tree inventory plot (Appendix A, Section 2.2.1). The individual tree records from the inventory dataset were then matched to ITC segments by

Table 2
Crown attributes computed from the ALS point cloud for each ITC segment. In bold, the attributes selected as predictors in the RF model.

Feature	Definition
HMAX (m)	Maximum crown height
HMEAN (m)	Mean crown height
HVAR	**Crown height variance**
HSD (m)	Crown height standard deviation
HKUR	Height kurtosis
HSKEW	Height skewness
CBH (m)	**Crown base height**
H5TH (m)	Crown height 5th percentile
H25TH (m)	**Crown height 25th percentile**
H50TH (m)	Crown height 50th percentile
H60TH (m)	Crown height 60th percentile
H70TH (m)	Crown height 70th percentile
H75TH (m)	Crown height 75th percentile
H80TH (m)	Crown height 80th percentile
H90TH (m)	Crown height 90th percentile
H95TH (m)	Crown height 95th percentile
H99TH (m)	Crown height 99th percentile
CL (m)	**Crown length (HMAX – CBH)**
CRAT	Crown ratio (CL/CBH)
CRAD (m)	**Crown Radius (sqrt(crown area/pi))**
CPA (m^2)	Simplified Crown Area (pi*CRAD^2)
CV (m^3)	Crown volume as the convex hull 3D
CSA (m^2)	Crown surface area as the convex hull 3D
CDS (%)	**Crown Density [(number of return ≥ CBH / total return)*100]**
CRT	HMAX -based crown ratio (100*CL/HMAX)
CFI	Crown form index (100*CL/ (2*CRAD))
CTI	Crown thickness index (100*(2*CRAD)/CL)
CSR	Crown spread ratio (100*(2*CRAD)/CBH)

minimizing a distance metric computed in a multi-dimensional space (Appendix A, Section 2.2.2). As a result, a total of 404 ITC segments were successfully linked to individual tree records and were used for training the RF model. Following Rocha et al. (2023), the most important predictors for the RF model were selected based on the correlation between the variables and the model improvement ratio (MIR), a standardized measure of variable importance (Evans and Murphy, 2018; Silva et al., 2017). The RF model was run in regression mode, and the number of random trees was set to 1000; the number of predictors considered at each node split was set at the default (p/3) in the 'randomForest' package, where p is the number of variables included in the model (Appendix A, Section 2.2.3).

Once the RF model was trained, foliage biomass was predicted for each crown delineated within the three study sites.

3.1.3. Annual tree leaf litter production

Annual tree crown leaf litterfall, i.e., the amount of foliage biomass annually shed by the tree (kg m^{-2} yr^{-1}), was estimated as a fraction of the crown foliage biomass, determined by the expected leaf turnover rate (He et al., 2012; Reinhardt, 2003; Tupek et al., 2015; White et al., 2000):

$$L_i = \frac{FB_i\ LTR_i}{CPA_i} \tag{1}$$

where L_i (kg m^{-2} yr^{-1}) is the annual tree leaf litterfall for tree crown *i*; FB_i (kg) is the estimated foliage biomass for the tree crown *i*; LTR_i (yr^{-1}) is the leaf turnover rate associated with crown *i*; and CPA_i is the crown projected area (m^2).

Leaf turnover rate (LTR) is the expected proportion of the foliage biomass that annually falls from a tree. It depends on tree species and environmental factors, with deciduous trees shedding the full foliage every year, whereas evergreen species retain a fraction of the foliage based on species, light, temperature, water, and nutrient availability (Holder, 2000; Jonasson, 1989; Kudo, 1992; Miyaji et al., 1997; Thomas and Stoddart, 1980). Since ALS data do not identify tree species, LTR_i was assigned to each crown based on the forest type map (Fig. 3) as the inverse of the expected leaf longevity of the dominant species (Holder, 2000; Schoettle et al., 1994; White et al., 2000).

In particular, the longleaf/slash pine group was the dominant forest type (Fig. 3). Holder (2000) reported large variability in needle lifespan of slash pine (1.28 – 1.95 years) and longleaf pine (0.58 – 2.49 years). Gholz et al. (1985) reported increases in needlefall with stand age up to 15 years, coinciding with the maximum of foliage biomass (Gholz and Fisher, 1982), and a decline of litterfall in old stands that parallels litter production. Based on these studies, we attributed higher LTR (lower lifespan) to slash and longleaf pine at Eglin AFB ($LTR = 0.58$ yr^{-1}, i.e., leaf life span $= 1.7$ yr) than ONF and PHP ($LTR_i = 0.45$ yr^{-1}, i.e., leaf life span $= 2.2$ yr), where stands were structurally more mature (Appendix A, Table A1 and A2). LTR_i for each tree crown *i* was assigned based on the raster cell (i.e., pixel) of the forest type map intersecting their centroid. If a tree crown was delineated on a pixel classified as non-forest, LTR_i was set to the predominant longleaf/slash pine forest type (Table 3).

Finally, the tree crown leaf litterfall estimates were rasterized at 5 m spatial resolution, which approximates the size of the dominant tree crown in this ecosystem (Loudermilk et al., 2011).

To account for the dispersion of litterfall from the tree due to wind, a convolution filter with a 3 × 3 kernel size was applied to the 5 m rasterized map. Higher litter accumulation is observed under or near tree crowns, and litter mass tends to decrease significantly 4 m from gap edges (Brockway and W. Outcalt, 1998). Therefore, making the conservative assumption that litter will mostly remain near each tree, we assigned a higher weight (2/3) to the focal pixel (center cell of the matrix) and distributed the remaining 1/3 uniformly among the remaining eight pixels, resulting in the following kernel matrix:

$$K = \begin{bmatrix} \frac{1}{24} & \frac{1}{24} & \frac{1}{24} \\ \frac{1}{24} & \frac{2}{3} & \frac{1}{24} \\ \frac{1}{24} & \frac{1}{24} & \frac{1}{24} \end{bmatrix} \tag{2}$$

In the final map, litterfall was estimated at each pixel location as:

$$L_x^f = \sum_{j=1}^{9} K_j L_j \tag{3}$$

where L_x^f is the final value of the tree leaf litter production in pixel x, K_j is the value of the kernel at location *j* in the 3 × 3 window, and L_j is the tree leaf litterfall estimated from the rasterization of Eq. (1) at location j in the 3 × 3 window centered on pixel *x*.

3.2. Tree leaf litter accumulation model

In this second step, we quantify tree leaf litter accumulation through a spatially explicit implementation of the Olson (1963) litter accumulation model using as model parameters the raster annual tree litterfall map (Section 3.1), decomposition rates estimated from MODIS actual evapotranspiration data (AET) (Fig. 4) (Gholz et al., 2000; Senay and Kagone, 2019), and the number of years since the last fire (YSF) compiled from fire history records (Fig. 5).

Table 3
Leaf turnover rates (LTR) attributed to the main forest types found in the study sites (Gholz et al., 1985; Holder, 2000; Schoettle et al., 1994).

Forest type	Group	LTR (yr^{-1})
Longleaf / slash pine	Softwood	0.45–0.58
Loblolly / shortleaf pine	Softwood	0.30
Oak / pine	Hardwood	0.75
Oak / hickory	Hardwood	1
Oak / gum / cypress	Hardwood	1

The Olson model is defined by two main parameters, the annual litter production (L) and the decomposition rate (k), and can be easily modified to consider litter that might remain unburnt after fire (Birk and Simpson, 1980; Zazali et al., 2020):

$$B(t) = \frac{L}{k}\left(1 - e^{-kt)}\right) + B^0 e^{-kt} \tag{4}$$

where $B(t)$ (kg m^{-2}) is the biomass accumulated at time t, L (kg m^{-2} yr^{-1}) is the annual litter production, k (yr^{-1}) is the decomposition rate, and B^0 (kg) is the litter at time $t = 0$ (i.e., the amount of litter not removed by the last fire).

In the absence of litter removal, a steady state is eventually reached when litter decomposition equals accumulation; peak accumulation B^{SS} (kg m^{-2}) can be expressed as:

$$B^{SS} = \frac{L}{k} \tag{5}$$

The Olson equation is an accumulation model well suited for stand-level and landscape analysis, but in the original formulation (Eq. (4)) it does not account for spatial heterogeneity. It is straightforward to write a spatially explicit version of the model:

$$B_x(t) = \frac{L_x}{k_x}\left(1 - e^{-k_x\left(t - T_x^0\right)}\right) + B_x^o e^{-k_x\left(t - T_x^0\right)} \tag{6}$$

where all the parameters of Eq. (4) are defined at each pixel location x, and T_x^0 is the time of the last known fire at each location.

Eq. (6) was used to estimate the biomass accumulation over the three study sites, with the relevant parameters set as follows:

- L_x: the annual litter production rate is obtained from Eq. (3) as the output of the annual litter production model (Section 3.1).
- k_x: the decomposition rate was estimated as a function of AET, through the regression model by Gholz et al. (2000) developed as part of the Long-term Intersite Decomposition Experiment (LIDET). LIDET was a litter-bag experiment that studied decomposition trends in several species across different sites in North and Central America, representing a wide variety of natural and managed ecosystems and climates, and provided species-specific equations for the decomposition rate. Our sites are dominated by pine species, where needles are the dominant leaf tissue. This litter has a larger lignin content and a smaller leaf specific area, so the decomposition rate is expected to be slower compared to deciduous dominated areas. The decomposition equation used was the linear model for pine leaves (Gholz et al., 2000):

$$k_x = 0.0139 + 0.0003\,\overline{AET}_x \tag{7}$$

where $\overline{AET}_x$ is the average annual evapotranspiration at the location x, calculated from the MODIS AET product (Section 2.2.4) resampled to 5 m resolution.

- T_x^0: the time of last fire was provided by the fire history records being T_x^0 the year of last fire. At locations where no fires were recorded within the timeframe covered by the fire records (i.e., no fire since 1972 at Eglin AFB, nor since 1996 at PHP), we assumed that the steady state accumulation was reached.
- B_x^o: litter at time T_x^o, i.e., litter remaining unburnt after last fire. In this case, it is based on the post-fire litter samples collected at Eglin AFB within the frame of the RxCADRE project (Ottmar et al., 2015). A constant value $B^0 = 0.04$ kg m^{-2} was used in all cases.

3.3. Accuracy assessment

The accuracy of the model was evaluated at two different levels, pixel and area, each comparing model estimates of tree leaf litter biomass with field measurements of litter biomass collected over the past two decades in the three study sites (Section 2.2.6). The year of the last fire was known at the time of the data collection, so the litter accumulation model (Eq. (6)) was re-run for each required YSF.

3.3.1. Pixel-level assessment

We assessed the accuracy of the model at the pixel-level by comparing litter biomass estimated on individual 5 m x 5 m pixels to field measurements with known clip plot geolocations (Table 1). Pixel-level assessment was performed at Eglin AFB and ONF, where the GPS coordinates of the clip plots were known.

At Eglin AFB, each validation point consisted of a clip plot measurement and the estimated litter biomass of the intersecting pixel of the accumulation map, totaling 262 observations (166 from the RxCADRE project, and 96 from the SERDP project). At ONF, the field sampling protocol was designed at a sub-pixel level (<5 m), since twelve clip plots were located within 4 m from a focal tree (Section 2.2.6). The average of these twelve samples was used as the observed field litter biomass at the location of each focal tree (Fig. 6) and the intersecting pixel as the estimated litter biomass value, resulting in 72 pixel-level observations.

The precision of the predictions was evaluated by computing the Root Mean Square Difference (RMSD):

$$RMSD = \sqrt{\frac{\sum_{i=1}^{n}\left(\widehat{Y}_i - Y_i\right)^2}{n}} \tag{8}$$

where n is the number of pixel-level measurements, Y_i is the field litter biomass (kg m^{-2}) measured for pixel i, and $\widehat{Y}_i$ is the litter biomass (kg m^{-2}) predicted in pixel i.

The accuracy of the predictions was evaluated by computing the bias:

$$BIAS = \frac{1}{n}\sum_{i=1}^{n}\left(\widehat{Y}_i - Y_i\right) \tag{9}$$

Note that litter samples collected at ONF only included litter from pine needles while our predictions accounted for all trees detected in the ALS data. The percentage of foliage biomass expected from deciduous trees was calculated from the tree inventory data using allometric equations (Appendix A, Table A3), resulting in a residual 1.1% that was considered negligible.

3.3.2. Area-level assessment

We also assessed the accuracy of the model at a raster multi-pixel level (hereinafter area-level assessment). In this case, litter areas enclosing several field litter clip plots were defined, and the average of the litter biomass measurements collected from the clip plots was compared to the average predicted litter biomass computed from all the pixels intersecting the perimeter of the litter area. Area-level assessment was performed at PHP and Eglin AFB using the litter biomass field measurements collected during the RxCADRE project. Note that the field sampling protocols at Eglin AFB in 2015 and at ONF in 2022 were designed at pixel and sub-pixel levels (≤5 m), and hence were excluded from the area-level assessment.

At Eglin AFB, 9 litter areas enclosing the 262 field litter clip plots were manually delineated around the clusters of the clip plots collected for the RxCADRE project (Hudak et al., 2015; Hudak and Bright, 2014). These litter clip plots were systematically placed within sub-units or along parallel transects at regular intervals defining a specific sampling extent (Section 2.2.6). The delineated extent ranged from 0.09 to 2.4 ha except for a larger defined litter area in the L2F unit (72.4 ha) that was delineated over the three parallel transects distributed at 100 m intervals over half of the management unit (Fig. 7).

At PHP, the litter areas consisted of the 24 research units (0.12 ha) in which litter was collected between 2006 and 2020 (Fig. 8). These areas were variously sampled at 1–6 YSF; therefore, a total of 68 replicates (research unit per YSF) were used for model assessment.

The precision and accuracy of the predictions at the area-level were again evaluated by computing RMSD and BIAS using Eqs. 8 and 9, with Y_i being the average litter biomass collected from the clip plots for each defined litter area i, and $\widehat{Y}_i$ being the average predicted litter biomass from all the pixels of the litter accumulation map intersecting the perimeter of litter area i.

Litter samples used for model assessment at PHP only included litter from pine needles. Around 12% of biomass within the A units would correspond to deciduous trees, 1% on the B units, and 9% on the C units. For model assessment on A and C units, we subtracted this percentage from the predicted litter average ($\widehat{Y}_i$).

The accuracy of the model was assessed in additional longleaf pine dominated forests of the North American Coastal Plain where field litter biomass measurements with known YSF and collocated with ALS data were available. These additional sites were JERC (Georgia), TTRS (Florida), Ft Stewart (Georgia), and Ft Jackson (South Carolina) (Appendix B, Figure B1). For a full description of the extended model assessment, including the field sampling protocols, model parametrization for each site, and accuracy assessment, refer to Appendix B.

4. Results

4.1. Tree leaf litter production

The percentage of variance explained by the RF model trained to predict tree crown foliage biomass was 57.7%. The crown attributes selected as predictors, in order of importance based on the mean decrease in accuracy, were CRAD (39.0%), CBH (28.8%), H25th (28.0%), HVAR (27.5%), CDS (17.6%), and CL (15.6%) (in bold in Table 2). Estimated average foliage biomass was 0.31 kg m^{-2} at Eglin AFB, 0.26 kg m^{-2} at PHP, and 0.57 kg m^{-2} at ONF. Fig. 9 exemplifies the foliage biomass estimated per crown and the resulting litter production maps for the three locations A, B, and C at PHP.

The average annual tree leaf litter production estimated with our crown-based model was 0.18 kg m^{-2} yr^{-1} at Eglin AFB, 0.11 kg m^{-2} yr^{-1} at PHP, and 0.26 kg m^{-2} yr^{-1} at ONF (Fig. 10).

4.2. Tree leaf litter accumulation

Predicted average decomposition (k) at Eglin AFB was 0.21 yr^{-1}, at PHP was 0.33 yr^{-1}, and at ONF was 0.40 yr^{-1}. There was a large spatial variability in decomposition rates within Eglin AFB reflecting $\overline{AET}_x$ ranging by an order of magnitude from 0.05 to 0.46 yr^{-1} across this largest study site (Fig. 4). Accordingly, the time necessary to reach 95% of the steady state of litter accumulation based on the Olson model at

Fig. 8. Research units (here litter areas) where litter was sampled at Pebble Hill Plantation (PHP) at the A, B, and C locations (Fig. 6) between 2006 and 2020.

Eglin AFB averaged ~16 years, while at PHP it was ~9 years, and at ONF it was ~7 years. Average predicted surface tree leaf litter in 2015 at Eglin AFB was 0.39 kg m^{-2}, in 2019 at PHP was 0.27 kg m^{-2}, and in 2022 at ONF was 0.44 kgm^{-2} (Fig. 11). Higher values result from the larger proportion of the area that is not frequently burned. Fig. 12 shows the estimated litter accumulation per time since fire for each of the study sites.

4.3. Model assessment

4.3.1. Pixel-level assessment

RMSD and BIAS were 0.21 and 0.01 kg m^{-2}, and the R Pearson correlation between predicted ($\widehat{Y}_i$) and observed (Y_i) values was 0.51 (Fig. 13, Table 4).

At Eglin AFB, RMSD of estimated litter loads was relatively similar compared to the two validation datasets (Table 4). Litter loads were underestimated compared to the RxCADRE measurements (BIAS = −0.06 kg m^{-2}) and, to a lesser degree, overestimated compared to the SERDP measurements (BIAS = 0.02 kg m^{-2}) (Fig. 13, Table 4). This pattern was expected since tree leaf litter was not separated from other tissue, such as bark, during the RxCADRE field data collection (Table 1). At ONF, the RMSD was only slightly worse than at Eglin AFB but litter loads were more positively biased (RMSD = 0.21 kg m^{-2}, BIAS = 0.14 kg m^{-2}) due mostly to the large overestimation at the unburned control units (Tables 4 and 5). Summarized by YSF, the contribution of the unburned units at ONF to the overall overestimation of litter loads is more apparent (Table 5).

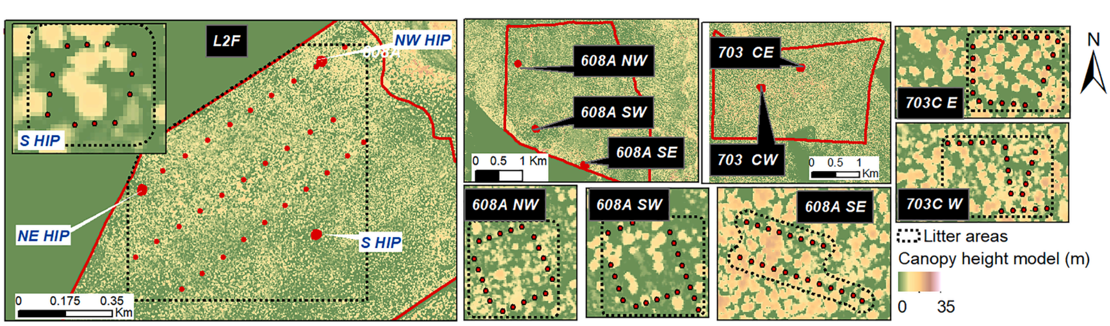

Fig. 7. Litter areas defined at Eglin AFB within the L2F, 608A, and 703C management units (Fig. 6) where litter was sampled in 2011 and 2012 during the RxCADRE project.

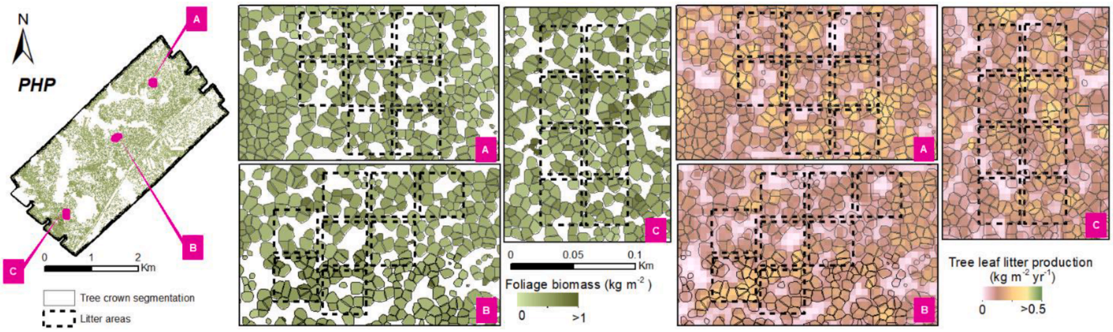

Fig. 9. Estimated foliage biomass density (left) and estimated annual tree leaf litter production (right) at the research units (here litter areas) at Pebble Hill Plantation (PHP). The tree crown segmentation is displayed to reference the tree locations. Foliage biomass density (kg m^{-2}) is calculated as the total estimated foliage biomass (kg) for each crown divided by the crown projected area (m^2).

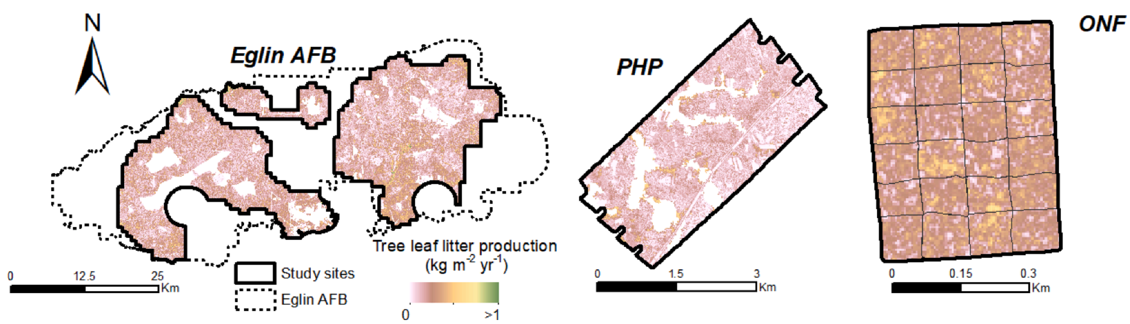

Fig. 10. Estimated annual tree leaf litter production at Eglin AFB, Pebble Hill Plantation (PHP), and Osceola National Forest (ONF).

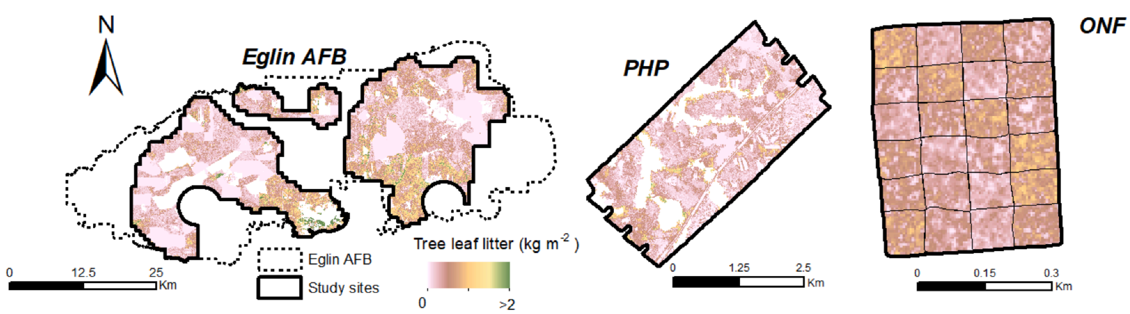

Fig. 11. Estimated tree leaf litter loads at Eglin AFB, Pebble Hill Plantation (PHP), and Osceola National Forest (ONF) in 2015, 2019, and 2022 respectively.

4.3.2. Area-level assessment

At the area-based level, RMSD and BIAS were 0.09 and 0.01 kg m^{-2}, and the R Pearson correlation between predicted ($\widehat{Y}_i$) and observed (Y_i) values was 0.73 (Fig. 14, Table 6).

By site, RMSD and BIAS were 0.09 and −0.05 kg m^{-2} at Eglin AFB, and 0.09 and 0.02 kg m^{-2} at PHP. At PHP, precision (RMSD) was better at the C unit than at the A or B units, while accuracy (BIAS) was better at the B and C units than at the A unit (Table 6).

Predicted litter loads were in good agreement with field-measured loads when stratified by YSF, as shown by the low observed BIAS up to the 6 years since fire (Table 7). The R Pearson correlation between predicted ($\widehat{Y}_i$) and observed (Y_i) values was high ($R > 0.75$) at 2 and 3 YSF, and moderate in all the other cases ($R \geq 0.40$). Note that the number of clip plots and litter areas available for evaluation decreases with YSF.

5. Discussion

Our newly developed modeling approach was successful for estimating spatially and temporally explicitly leaf litter accumulation and distribution mainly driven by tree foliage biomass and time since the last fire. Previous studies already showed a relationship between litter loads and overlying tree foliage and/or time since last disturbance (Bright et al., 2022; Dunn and Bailey, 2015; Eskelson and Monleon, 2018; Hudak et al., 2016; Lydersen et al., 2015; Stevens-Rumann et al., 2020). For instance, Hudak et al. (2016) reported high correlation between surface fuel loads, ALS canopy-related variables, and YSF at Eglin AFB. Also, Bright et al. (2022) predicted surface fuels with ALS data showing a non-linear accumulation pattern as is described by the Olson model. The Bright et al. (2022) study was conducted on the Kaibab Plateau of Arizona and another study by Boisramé et al. (2022) spanned the entire western U.S., where fire return intervals are slower (decadal), yet the functional form of the relationship to YSF is the same. We demonstrated in this study that canopy litter inputs and YSF are two major drivers of accumulation in fire-maintained longleaf pine forests of the southeastern US, especially during the first few years following fire. We also demonstrated that the proposed model, based on tree crown objects derived from ALS data, provides a means to characterize spatially explicit litterfall patterns and the discontinuity of the litter layer conditioned on the overstory, such that the resulting heterogeneity

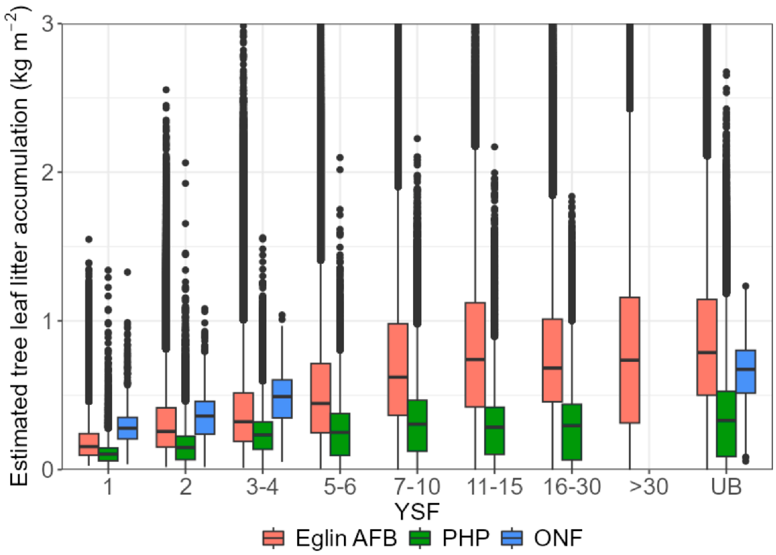

Fig. 12. Boxplots of the estimated tree leaf litter accumulation (kg m^{-2}) based on the year since fire (YSF) of the maps displayed in Fig. 11. UB: unburnt; YSF = 0 not displayed; 0.3% of the 5 m pixel values of the tree leaf litter accumulation map that had litter biomass larger than 3 kg m^{-2} are not displayed on the graph.

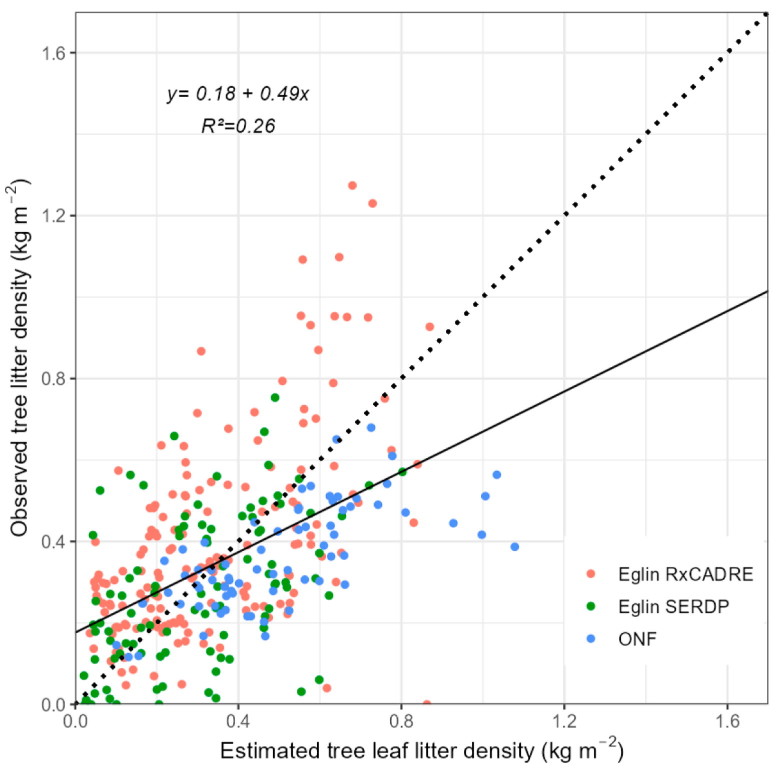

Fig. 13. Observed tree litter (kg m^{-2}) of the 334 pixel-level measurements made at Eglin AFB (during RxCADRE and SERDP projects) and Osceola National Forest (ONF) (y axis), and estimated tree leaf litter (kg m^{-2}) of the intersecting pixels of the accumulation map (x axis). The dashed line represents the 1:1 relationship, and the solid line represents the linear regression ($y = \beta_0 + \beta_1$x).

Table 4
Average observed tree litter (kg m^{-2}) and average estimated tree leaf litter (kg m^{-2}) of the 334 pixel-level measurements made at Eglin AFB and Osceola National Forest (ONF); n_p indicates the number of pixel-level measurements evaluated at each site based on independent field validation datasets. Intercept (β_0) and slope (β_1) of the linear regression between the field-based (y) and estimated litter loads (x), Pearson's correlation (R), root mean square difference (RMSD), and BIAS.

Site	Dataset	n_p	$avg(Y_i)$ (kg m^{-2})	$avg(\widehat{Y}_i)$ (kg m^{-2})	β_0	β_1	R	RMSD (kg m^{-2})	BIAS (kg m^{-2})
Eglin AFB	RxCADRE	166	0.39	0.34	0.18	0.64	0.55	0.22	−0.06
	SERDP	96	0.28	0.30	0.15	0.45	0.46	0.19	0.02
ONF	Burns 2022	72	0.36	0.50	0.16	0.40	0.70	0.21	0.14
All	**All**	**334**	**0.35**	**0.36**	**0.18**	**0.49**	**0.51**	**0.21**	**0.01**

Table 5
Average observed tree litter (kg m^{-2}) and average estimated tree leaf litter (kg m^{-2}) of the 334 pixel-level measurements made at Eglin AFB and Osceola National Forest (ONF) per year since fire (YSF); n_p indicates the number of pixel-level measurements evaluated per YSF. Intercept (β_0) and slope (β_1) of the linear regression between the field-based (y) and estimated litter loads (x), Pearson's correlation (R), root mean square difference (RMSD), and BIAS. UB: unburnt.

YSF	n_p	$avg(Y_i)$ (kg m^{-2})	$avg(\widehat{Y}_i)$ (kg m^{-2})	β_0	β_1	R	RMSD (kg m^{-2})	BIAS (kg m^{-2})
1	18	0.27	0.31	0.20	0.21	0.32	0.11	0.04
2	214	0.31	0.31	0.17	0.42	0.48	0.18	0.01
3	66	0.48	0.37	0.16	0.87	0.60	0.27	−0.11
4	18	0.43	0.56	0.23	0.37	0.52	0.16	0.13
UB	18	0.48	0.74	0.43	0.07	0.13	0.34	0.27

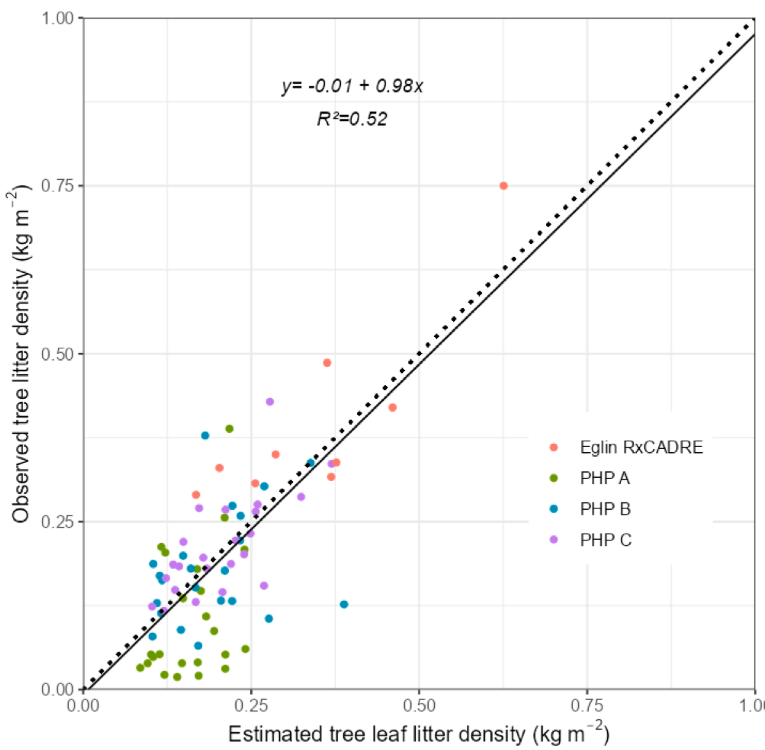

Fig. 14. Average observed tree litter (kg m^{-2}) of the 77 defined litter areas at Eglin AFB and Pebble Hill Plantation (PHP) (y axis), and average estimated tree leaf litter (kg m^{-2}) of all the pixels of the litter accumulation map intersecting the same litter areas (x axis). The dashed line represents the 1:1 relationship, and the solid line represents the linear regression ($y = \beta_0 + \beta_1 x$).

Table 6
Average observed tree litter (kg m^{-2}) and average estimated tree leaf litter (kg m^{-2}) of the 77 litter areas (n_{la}) defined at Eglin AFB and Pebble Hill Plantation (PHP); n_p indicates the number of clip plot measurements per site and dataset. Intercept (β_0) and slope (β_1) of the linear regression between the field-based (y) and estimated litter loads (x), Pearson's correlation (R), root mean square difference (RMSD), and BIAS.

Site	Dataset/Location	n_{la}	n_p	$avg(Y_i)$ (kg m^{-2})	$avg(\widehat{Y}_i)$(kg m^{-2})	β_0	β_1	R	RMSD (kg m^{-2})	BIAS (kg m^{-2})
Eglin AFB	RxCADRE	9	166	0.40	0.35	0.09	0.88	0.85	0.09	−0.05
PHP	A	23	252	0.11	0.16	−0.01	0.72	0.36	0.10	0.05
	B	22	221	0.18	0.19	0.11	0.37	0.34	0.09	0.01
	C	23	286	0.21	0.21	0.06	0.75	0.70	0.06	−0.01
All	**All**	**77**	**925**	**0.19**	**0.20**	**−0.01**	**0.98**	**0.73**	**0.09**	**0.01**

matches field observations fairly well.

Our leaf litter accumulation estimates showed a significantly low BIAS up to 4 YSF, which suggest that the litterfall inputs included on the spatially explicit implementation of the Olson model were within the expected range. Our annual litter production averages (0.11–0.26 kg m^{-2} yr^{-1}) were lower than published measurements obtained with field traps in similar forest regions, which generally ranged from 0.3 to 0.6 kg m^{-2} yr^{-1} depending on species, maturity, and site index (e.g., Gholz et al., 1985; Gresham, 1982; Haywood et al., 1995; Wiegert and Monk, 1972). However, it should be noted that our estimates are averaged over large areas including gaps and low tree canopy cover, so they are not directly comparable with measurements collected through field traps which are typically placed in points with high tree canopy cover. Our explicit consideration of discontinuity in surface fuelbed development is a central contribution of our study. Furthermore, the moderate to high correlation between predicted and observed litter biomass loads (Tables 4–7) is notable considering the high local heterogeneity on the forest floor (Table 1), and the difference in size between the litter clip plots (0.09–1 m^2) and the raster pixel size of the leaf litter accumulation map (25 m^2).

Our results also indicate that the lack of individual tree species maps for the entire extent of the study sites was a significant source of

Table 7
Average observed tree litter (kg m^{-2}) and average estimated tree leaf litter (kg m^{-2}) of the 77 litter areas (n_{la}) defined at Eglin AFB and Pebble Hill Plantation (PHP) per year since fire (YSF); n_p indicates the number of clip plot measurements per YSF. Intercept (β_0) and slope (β_1) of the linear regression between the field-based (y) and estimated litter loads (x), Pearson's correlation (R), root mean square difference (RMSD), and BIAS.

YSF	n_{la}	n_p	$avg(Y_i)$ (kg m^{-2})	$avg(\hat{Y}_i)$ (kg m^{-2})	β_0	β_1	R	RMSD (kg m^{-2})	BIAS (kg m^{-2})
1	21	300	0.13	0.12	−0.03	1.33	0.44	0.05	−0.01
2	23	304	0.20	0.21	−0.00	0.94	0.76	0.07	0.01
3	19	221	0.26	0.26	−0.07	1.30	0.80	0.11	−0.01
4	9	58	0.18	0.26	0.05	0.49	0.40	0.12	0.08
5	4	36	0.22	0.25	−0.55	3.13	0.61	0.13	0.02
6	1	6	0.26	0.23	–	–	–	0.02	−0.02

uncertainty. The 30 m resolution forest group map was too coarse to fully characterize the variability of the forest composition at the study sites, especially given the localized extents of our assembled calibration datasets. For instance, the larger discrepancies between observed and predicted values in the A research units compared to the B and C units at PHP could be explained by the higher proportion of shortleaf pines in unit A, whereas the forest type group map (Fig. 3) indicates that the longleaf/slash group is the prevalent type. The availability of individual tree species maps would also facilitate further development of the proposed model, allowing for the characterization of litter structure. For instance, longleaf pine trees tend to create an aerated fuel bed of needles, some suspended in the herbaceous and shrub understory vegetation, whereas shortleaf pine needles are much more likely to accumulate densely on the forest floor (Reid and Robertson, 2012). Data fusion between ALS and high resolution optical data are promising avenues for the generation of wall-to-wall tree species maps (Ferreira et al., 2020; Hartling et al., 2019; Mäyrä et al., 2021; Shi et al., 2018), and it will be investigated in the context of future improvements to the proposed model.

Furthermore, year-to-year studies of needlefall and leaf lifespan in pine forests show that litter production is not a steady process in time or space (e.g., Gholz et al., 1985; Holder, 2000; Liu et al., 2004; Wiegert and Monk, 1972). Holder (2000) studied the leaf lifespan of longleaf and slash pines in five locations in the southeastern US and reported large plasticity, especially in longleaf pine (0.58–2.49 years compared to slash pine's range of 1.28–1.95 years). Wiegert and Monk (1972) studied litterfall dynamics in three forest stands of longleaf pine of different ages (7, 11, and 13-years). They observed that approximately 50% of the needles were recovered as litterfall each year, but there was variability among sites, ranging from 29% in the 7-year to 86% in the 11-year stands. Climate and weather variability could induce periods of stress in which foliage production slows down and/or litterfall is promoted due to nutrient deficits and sudden events (e.g., hurricanes, windstorms, insect infestations, or crown scorch from previous fire). Besides this, our litter distribution approach based on the convolution filter assumes that litter mostly remains under the tree canopy, and evenly disperses to neighboring cells. However, both prevailing winds and topographic slope could cause anisotropic patterns of accumulation.

Fire regimes induce changes in decomposer activity by affecting fungal and microbial communities (Brennan et al., 2009; Butler et al., 2019; Dao et al., 2022; Fox et al., 2022; Hopkins et al., 2020; Semenova-Nelsen et al., 2019), but the pathways linking these processes are still poorly understood. Impacts could differ under the presence of fire-adapted organisms or under different fire intensities (Hopkins et al., 2020). Butler et al. (2019) reported faster microbial decomposition on unburned treatments compared to sites burnt every 2 and 4 years; however, they also indicated that invertebrate activity compensated for the microbial depletion to inhibit decomposition in these frequently burnt areas. Semenova-Nelsen et al. (2019) reported a 6.5%, 11%, and 13% difference in litter mass loss after 3-, 6-, and 9-months following fire on litter samples collected in recently burned and less recently burned longleaf pine forest. Previous measurements at the Stoddard Fire Plots at TTRS in the organic matter turnover was more than twice as high in unburned than in the frequently burned (1–3 year interval) plots (Godwin et al., 2017). We speculate that changes in decomposition might also explain some of the patterns observed in our results. For instance, field data collected at PHP shows a decrease in litter accumulation after 3 YSF (Table 1). The field samples were not geolocated within the research units, and the number of samples with YSF>3 was low, such that this trend could be attributed to undersampling. However, this result and the overestimation of litter loads in the 4 YSF and unburnt units at ONF do suggest an increase in decomposition rate after a few years since fire. The development of deeper litter (and eventually duff) layers could absorb more moisture and promote more microbial activity, and microbial communities presumably become increasingly established in the litter and duff layer with time since fire (Semenova-Nelsen et al., 2019). Therefore, a two- or multi-phase litter decomposition model, as opposed to the one phase used in our implementation of the Olson model, might improve the estimates of litter loads with increasing time since fire (Harmon et al., 2009; Zazali et al., 2020).

Given the short return interval of prescribed fires in the ecosystems studied, information on the complete fuel life cycle, including consumption during fires, decomposition between fires, and resulting fuel loads at time of fire, is important to better predict fuel load dynamics over multiple fire intervals. The Olson model, as originally proposed, assumed that litter was not initially present on the forest floor. In contrast, empirical studies report that a significant proportion of litter, as much as half, remains unburned, especially after prescribed fires (Hudak et al., 2020; Ottmar et al., 2015; Reid et al., 2012). While we accounted for unburned biomass, we used a constant B^0 value, based on post-fire litter samples collected at Eglin AFB during the RxCADRE project (Ottmar et al., 2015; Ottmar and Restaino, 2014). This constant value might explain the lower correlation between predicted and observed values in the first year after fire compared to the second and third year, even though the average values were similar (Table 7). Future research will investigate whether the fraction of unburned litter could also be mapped, either through monitoring the fire behavior and assessing fuel consumption using tools such as thermal remote sensing data, or investigating whether local fuel consumption may be driven by the same tree clustering patterns that determine the heterogeneity imposed by our spatially explicit model.

The above limitations notwithstanding, the results demonstrate that the proposed model is able to generate spatially and temporally explicit estimates of tree litter fuel load accumulation in environments subject to frequent surface fires at 5 m resolution and annual time steps. Such information is currently missing for most forested sites: previously proposed methods, including ecological-based models and data-driven techniques, do not account for the spatial and temporal variability of the litter bed. Collating input litterfall information through traditional field sampling methods is time-consuming and expensive, and it does not provide wall-to-wall information. The use of ALS data and new techniques of image segmentation to estimate expected litterfall rates at the tree crown level largely overcomes this limitation. Our model also outperforms empirical data-driven approaches that use surface fuel data for training models (e.g., Bright et al., 2022; Lydersen et al., 2015). The transferability of those models is limited by the amount of data required to represent the tremendous heterogeneity of fuels (Keane, 2015, 2008; Keane et al., 2013, 2012, 2001; Keane and Gray, 2013). In contrast, our model did not require litter biomass measurements. Rather, we estimated foliage biomass using tree inventory data which is more widely available and easier to collect, it is less prone to undersampling, and it is more consistent between sites. As a result, our model is transferable among Coastal Plain longleaf pine forests, as demonstrated by the consistency of the results at all evaluated sites, including other sites in the extended model assessment (Appendix B). The workflow can also be adjusted to sites dominated by different tree species and environmental conditions. Our approach can provide annually updated maps of litter loads to forest managers. Many available products providing information on surface fuels are static maps based on fuelbed or vegetation types (e.g., those derived from the fuel characteristics classification system, FCCS). By incorporating fire history maps, we assert that litter loads can be dynamically updated on an annual basis.

6. Conclusions

This model illustrates a novel yet simple methodology to quantify the spatially explicit litter loads in longleaf pine forests in the southeastern US that are managed using frequent prescribed fires. Our goal and achievement were twofold. First, we leveraged our understanding of the litter accumulation process combining traditional ecological-based modeling with up-to-date machine learning and remote sensing techniques for wall-to-wall mapping of litter fuels over relatively large areas. Second, we demonstrated that aboveground biomass and YSF are the two major drivers of tree leaf litter accumulation in these fire-maintained longleaf pine forests, especially during the first years following fire. Therefore, spatially explicit information on these two parameters could be sufficient for a generalized characterization of the accumulation process in a heterogeneous manner that reflects overstory canopy controls on surface fuel accumulation. This methodology provides realistic estimates of litter fuels and, where ALS is available, partially resolves the challenge of wall-to-wall mapping of the highly heterogeneous distribution of litter over the forest floor. Therefore, the model overcomes many of the spatial limitations of traditional ecological landscape models and current data-driven modeling approaches.

This integrated modeling approach is a step toward meeting the greater challenge of characterizing spatial patterns of multiple fuel components, including duff, woody debris, herbs, and shrubs at high spatial resolution that better matches the fine scales at which wildland fuel beds vary. Where other modeling approaches may fail to provide the resolution and accuracy managers need, models such as presented in this study can fill the information gap. These maps will improve decision-making involving application of prescribed fire for accomplishing ecological and natural resource management goals.

CRediT author statement

All authors have read and agreed to the published version of the manuscript.

CRediT authorship contribution statement

Nuria Sánchez-López: Conceptualization, Methodology, Formal analysis, Software, Validation, Investigation, Writing – original draft, Writing – review & editing, Visualization. **Andrew T. Hudak:** Conceptualization, Methodology, Investigation, Resources, Writing – original draft, Writing – review & editing, Supervision, Funding acquisition. **Luigi Boschetti:** Conceptualization, Methodology, Writing – original draft, Writing – review & editing, Supervision. **Carlos A. Silva:** Software, Writing – review & editing. **Kevin Robertson:** Resources, Writing – review & editing. **E Louise Loudermilk:** Resources, Writing – review & editing. **Benjamin C. Bright:** Software, Writing – review & editing. **Mac A. Callaham:** Resources, Writing – review & editing. **Melanie K. Taylor:** Resources, Writing – review & editing.

Declaration of Competing Interest

The authors declare the following financial interests/personal relationships which may be considered as potential competing interests:

Nuria Sánchez López reports financial support was provided by Strategic Environmental Research and Development Program.

Data availability

There are several datasets used on the manuscript. Some data is already publicly available, and the authors will make available under request the datasets they have permission on.

Acknowledgements

Funding was provided by the Department of Defense (DOD) Strategic Environmental Research and Development Program (SERDP) award RC20–1346 to the US Forest Service Rocky Mountain Research Station, and a subaward to the University of Idaho through Joint Venture Agreement 20-JV-11221633–154.

This research was supported by the U.S. Department of Agriculture, Forest Service, Rocky Mountain Research Station. The findings and conclusions in this publication are those of the authors and should not be construed to represent any official USDA or U.S. Government determination or policy.

We would like to express our sincere gratitude to Eglin AFB and Jackson Guard, the Pebble Hill Foundation, the forest managers at ONF, TTRS, Ft Stewart, Ft Jackson, and JERC for granting access to the field sites, providing logistical assistance and/or sharing their fire history records and additional field datasets as required, and for maintaining fire treatments and prescribed management plans. We thank all the field crews and technicians who contributed to the several field data collections over the years. The availability of these datasets from past projects and research campaigns made this study possible. Finally, we extend our thanks to the anonymous Reviewers for their feedback and time invested in our manuscript.

Supplementary materials

Supplementary material associated with this article can be found, in the online version, at doi:10.1016/j.ecolmodel.2023.110369.

References

Agee, J.K., Skinner, C.N., 2005. Basic principles of forest fuel reduction treatments. For. Ecol. Manage. 211, 83–96.

Bezkorovaynaya, I.N., 2005. The formation of soil invertebrate communities in the Siberian afforestation experiment. Tree Species Effects On Soils: Implications for Global Change. Springer, pp. 307–316.

Birk, E.M., Simpson, R.W., 1980. Steady state and the continuous input model of litter accumulation and decompostion in Australian eucalypt forests. Ecology 61, 481–485. https://doi.org/10.2307/1937411.

Boisramé, G.F., Brown, T.J., Bachelet, D.M., 2022. Trends in western USA fire fuels using historical data and modeling. Fire Ecol. 18, 1–34.

Bond, W.J., Woodward, F.I., Midgley, G.F., 2005. The global distribution of ecosystems in a world without fire. New Phytol. 165, 525–538. https://doi.org/10.1111/j.1469-8137.2004.01252.x.

Brennan, K.E.C., Christie, F.J., York, A., 2009. Global climate change and litter decomposition: more frequent fire slows decomposition and increases the functional importance of invertebrates. Glob. Chang. Biol. 15, 2958–2971. https://doi.org/10.1111/j.1365-2486.2009.02011.x.

Breiman, L., 2001. Random forests. Mach. Learn. 45, 5–32. 10.1023/A:1010933404324.

Bright, B.C., Hudak, A.T., McCarley, T.R., Spannuth, A., Sánchez-López, N., Ottmar, R.D., Soja, A.J., 2022. Multitemporal lidar captures heterogeneity in fuel loads and consumption on the Kaibab Plateau. Fire Ecol. 18, 18. https://doi.org/10.1186/s42408-022-00142-7.

Brockway, D.G., Outcalt, W., 1998. Gap-phase regeneration in longleaf pine wiregrass ecosystems. For. Ecol. Manage. 106, 125–139. https://doi.org/10.1016/S0378-1127(97)00308-3.

Butler, O.M., Lewis, T., Rezaei Rashti, M., Maunsell, S.C., Elser, J.J., Chen, C., 2019. The stoichiometric legacy of fire regime regulates the roles of micro-organisms and invertebrates in decomposition. Ecology 100, e02732. https://doi.org/10.1002/ecy.2732.

Carr, S.C., Robertson, K.M., Peet, R.K., 2010. A vegetation classification of fire-dependent pinelands of Florida. Cast 75, 153–189. https://doi.org/10.2179/09-016.1.

Chen, Q., Gong, P., Baldocchi, D., Tian, Y.Q., 2007. Estimating basal area and stem volume for individual trees from lidar data. Photogramm. Eng. Remote Sensing 73, 1355.

Costa, A.N., Souza, J.R., Alves, K.M., Penna-Oliveira, A., Paula-Silva, G., Becker, I.S., Marinho-Vieira, K., Bonfim, A.L., Bartimachi, A., Vieira-Neto, E.H.M., 2020. Linking the spatiotemporal variation of litterfall to standing vegetation biomass in Brazilian savannas. J. Plant Ecol. 13, 517–524. https://doi.org/10.1093/jpe/rtaa039.

Dao, V.Q., Potts, S.E., Johnson, C.N., Sikes, B.A., Platt, W.J., 2022. Substrate and low intensity fires influence bacterial communities in longleaf pine savanna. Sci. Rep. 12, 20904.

Dunn, C.J., Bailey, J.D., 2015. Temporal fuel dynamics following high-severity fire in dry mixed conifer forests of the eastern Cascades, Oregon, USA. Int. J. Wildland Fire 24, 470–483.

Eskelson, B.N., Monleon, V.J., 2018. Post-fire surface fuel dynamics in California forests across three burn severity classes. Int. J. Wildland Fire 27, 114–124.

Evans, J.S., Murphy, M.A., 2018. rfUtilities. R package version 2.1-3. https://cran.r-project.org/web/packages/rfUtilities.

Eysn, L., Hollaus, M., Lindberg, E., Berger, F., Monnet, J.-.M., Dalponte, M., Kobal, M., Pellegrini, M., Lingua, E., Mongus, D., 2015. A benchmark of lidar-based single tree detection methods using heterogeneous forest data from the alpine space. Forests 6, 1721–1747.

Ferrari, J.B., Sugita, S., 1996. A spatially explicit model of leaf litter fall in hemlock–hardwood forests. Can. J. For. Res. 26, 1905–1913. https://doi.org/10.1139/x26-215.

Ferreira, M.P., de Almeida, D.R.A., de Almeida Papa, D., Minervino, J.B.S., Veras, H.F.P., Formighieri, A., Santos, C.A.N., Ferreira, M.A.D., Figueiredo, E.O., Ferreira, E.J.L., 2020. Individual tree detection and species classification of Amazonian palms using UAV images and deep learning. For. Ecol. Manage. 475, 118397.

FNAI, 2010. Guide to the natural communities of Florida: 2010 edition. Fla. Nat. Areas Inventory Tallahass. FL.

Fox, S., Sikes, B.A., Brown, S.P., Cripps, C.L., Glassman, S.I., Hughes, K., Semenova-Nelsen, T., Jumpponen, A., 2022. Fire as a driver of fungal diversity—A synthesis of current knowledge. Mycologia 114, 215–241.

Gholz, H.L., Fisher, R.F., 1982. Organic matter production and distribution in Slash Pine (Pinus Elliottii) plantations. Ecology 63, 1827–1839. https://doi.org/10.2307/1940124.

Gholz, H.L., Perry, C.S., Cropper Jr., W.P., Hendry, L.C., 1985. Litterfall, decomposition, and nitrogen and phosphorus dynamics in a chronosequence of slash pine (Pinus elliottii) plantations. Forest Science 31, 463–478. https://doi.org/10.1093/forestscience/31.2.463.

Gholz, H.L., Wedin, D.A., Smitherman, S.M., Harmon, M.E., Parton, W.J., 2000. Long-term dynamics of pine and hardwood litter in contrasting environments: toward a global model of decomposition. Glob. Chang. Biol. 6, 751–765.

Godwin, D.R., Kobziar, L.N., Robertson, K.M., 2017. Effects of fire frequency and soil temperature on soil CO2 efflux rates in old-field pine-grassland forests. Forests 8, 274.

Gonzalez-Benecke, C.A., Gezan, S.A., Albaugh, T.J., Allen, H.L., Burkhart, H.E., Fox, T.R., Jokela, E.J., Maier, C.A., Martin, T.A., Rubilar, R.A., 2014. Local and general above-stump biomass functions for loblolly pine and slash pine trees. For. Ecol. Manage. 334, 254–276.

Gonzalez-Benecke, C.A., Zhao, D., Samuelson, L.J., Martin, T.A., Leduc, D.J., Jack, S.B., 2018. Local and general above-ground biomass functions for Pinus palustris trees. Forests 9, 310.

Grace, S.L., Platt, W.J., 1995. Effects of adult tree density and fire on the demography of pregrass stage juvenile longleaf pine (Pinus palustris Mill.). J. Ecol. 75–86.

Gresham, C.A., 1982. Litterfall patterns in mature loblolly and longleaf pine stands in coastal South Carolina. For. Sci. 28, 223–231. https://doi.org/10.1093/forestscience/28.2.223.

Harmon, M.E., Silver, W.L., Fasth, B., Chen, H.U.A., Burke, I.C., Parton, W.J., Hart, S.C., Currie, W.S., Lidet, 2009. Long-term patterns of mass loss during the decomposition of leaf and fine root litter: an intersite comparison. Glob. Chang. Biol. 15, 1320–1338.

Hartling, S., Sagan, V., Sidike, P., Maimaitijiang, M., Carron, J., 2019. Urban tree species classification using a WorldView-2/3 and LiDAR data fusion approach and deep learning. Sensors 19, 1284.

Haywood, J.D., Tiarks, A.E., Elliott-Smith, M.L., Pearson, H.A., 1995. Management of longleaf stands for pine straw harvesting and the subsequent influence on forest productivity. In: Proceedings of the Eighth Biennial South. Silv. Res. Conf. USDA For. Serv. Gen. Tech. Rep. SRSGTR-1, pp. 281–287.

He, L., Chen, J.M., Pan, Y., Birdsey, R., Kattge, J., 2012. Relationships between net primary productivity and forest stand age in US forests. Glob. Biogeochem. Cycles 26.

Hiers, J.K., O'Brien, J.J., Mitchell, R.J., Grego, J.M., Loudermilk, E.L., 2009. The wildland fuel cell concept: an approach to characterize fine-scale variation in fuels and fire in frequently burned longleaf pine forests. Int. J. Wildland Fire 18, 315–325.

Holder, C.D., 2000. Geography of Pinus elliottii Engelm. and Pinus palustris Mill. leaf life-spans in the southeastern USA. J. Biogeogr. 27, 311–318.

Hopkins, J.R., Huffman, J.M., Platt, W.J., Sikes, B.A., 2020. Frequent fire slows microbial decomposition of newly deposited fine fuels in a pyrophilic ecosystem. Oecologia 193, 631–643.

Hudak, A.T., Bright, B.C., 2014. RxCADRE 2008, 2011, and 2012: Clip Plot Locations. Forest Service Research Data Archive, Fort Collins, CO. https://doi.org/10.2737/RDS-2014-0030.

Hudak, A.T., Bright, B.C., Pokswinski, S.M., Loudermilk, E.L., O'Brien, J.J., Hornsby, B. S., Klauberg, C., Silva, C.A., 2016. Mapping forest structure and composition from low-density LiDAR for informed forest, fuel, and fire management at Eglin Air Force Base, Florida, USA. Can. J. Remote Sens. 42, 411–427. https://doi.org/10.1080/07038992.2016.1217482.

Hudak, A.T., Dickinson, M.B., Bright, B.C., Kremens, R.L., Loudermilk, E.L., O'Brien, J.J., Hornsby, B.S., Ottmar, R.D., 2015. Measurements relating fire radiative energy density and surface fuel consumption–RxCADRE 2011 and 2012. Int. J. Wildland Fire 25, 25–37.

Hudak, A.T., Kato, A., Bright, B.C., Loudermilk, E.L., Hawley, C., Restaino, J.C., Ottmar, R.D., Prata, G.A., Cabo, C., Prichard, S.J., Rowell, E.M., Weise, D.R., 2020. Towards spatially explicit quantification of pre- and postfire fuels and fuel consumption from traditional and point cloud measurements. For. Sci. 66, 428–442. https://doi.org/10.1093/forsci/fxz085.

Isenburg, M., 2021. LAStools - efficient LiDAR processing software (version 201124, academic), https://rapidlasso.com/lastools/ (last accessed 7/3/2022).

Jakubowski, M.K., Li, W., Guo, Q., Kelly, M., 2013. Delineating individual trees from lidar data: a comparison of vector- and raster-based segmentation approaches. Remote Sens. (Basel) 5, 4163–4186. https://doi.org/10.3390/rs5094163.

Jevon, F.V., Polussa, A., Lang, A.K., William Munger, J., Wood, S.A., Wieder, W.R., Bradford, Mark.A., 2022. Patterns and controls of aboveground litter inputs to temperate forests. Biogeochemistry. https://doi.org/10.1007/s10533-022-00988-8.

Jonasson, S., 1989. Implications of leaf longevity, leaf nutrient re-absorption and translocation for the resource economy of five evergreen plant species. Oikos 121–131.

Keane, R.E., 2012. Describing wildland surface fuel loading for fire management: a review of approaches, methods and systems. Int. J. Wildland Fire 22, 51–62. https://doi.org/10.1071/WF11139.

Keane, R.E., 2008. Biophysical controls on surface fuel litterfall and decomposition in the northern Rocky Mountains, USA. Can. J. For. Res. 38, 1431–1445.

Keane, R.E., 2015. *Wildland fuel fundamentals and applications* (No. 11904). Springer International Publishing, Cham, Switzerland.

Keane, R.E., Burgan, R., van Wagtendonk, J., 2001. Mapping wildland fuels for fire management across multiple scales: integrating remote sensing, GIS, and biophysical modeling. Int. J. Wildland Fire 10, 301–319.

Keane, R.E., Gray, K., 2013. Comparing three sampling techniques for estimating fine woody down dead biomass. Int. J. Wildland Fire 22, 1093–1107.

Keane, R.E., Gray, K., Bacciu, V., Leirfallom, S., 2012. Spatial scaling of wildland fuels for six forest and rangeland ecosystems of the northern Rocky Mountains, USA. Landsc. Ecol. 27, 1213–1234.

Keane, R.E., Herynk, J.M., Toney, C., Urbanski, S.P., Lutes, D.C., Ottmar, R.D., 2013. Evaluating the performance and mapping of three fuel classification systems using forest inventory and analysis surface fuel measurements. For. Ecol. Manage. 305, 248–263.

Khosravipour, A., Skidmore, A.K., Isenburg, M., Wang, T., Hussin, Y.A., 2014. Generating pit-free canopy height models from airborne lidar. Photogramm. Eng. Remote Sens. 80, 863–872.

Kirkman, L.K., Mitchell, R.J., Helton, R.C., Drew, M.B., 2001. Productivity and species richness across an environmental gradient in a fire-dependent ecosystem. Am. J. Bot. 88, 2119–2128.

Krishna, M.P., Mohan, M., 2017. Litter decomposition in forest ecosystems: a review. Energy, Ecol. Environ. 2, 236–249.

Kudo, G., 1992. Effect of snow-free duration on leaf life-span of four alpine plant species. Can. J. Botany 70, 1684–1688.

Li, W., Guo, Q., Jakubowski, M.K., Kelly, M., 2012. A new method for segmenting individual trees from the lidar point cloud. Photogramm. Eng. Remote Sens. 78, 75–84.

Liaw, A, Wiener, M, 2002. Classification and Regression by randomForest. R News 2 (3), 18–22. https://CRAN.R-project.org/doc/Rnews/.

Liu, C., Westman, C.J., Berg, B., Kutsch, W., Wang, G.Z., Man, R., Ilvesniemi, H., 2004. Variation in litterfall-climate relationships between coniferous and broadleaf forests in Eurasia. Glob. Ecol. Biogeogr. 13, 105–114.

Loomis, R.M., Phares, R.E., Crosby, J.S., 1966. Estimating foliage and branchwood quantities in shortleaf pine. For. Sci. 12, 30–39.

Loudermilk, E.L., Cropper, W.P., Mitchell, R.J., Lee, H., 2011. Longleaf pine (Pinus palustris) and hardwood dynamics in a fire-maintained ecosystem: a simulation approach. Ecol. Modell. 222, 2733–2750. https://doi.org/10.1016/j.ecolmodel.2011.05.004.

Loudermilk, E.L., O'Brien, J.J., Mitchell, R.J., Cropper, W.P., Hiers, J.K., Grunwald, S., Grego, J., Fernandez-Diaz, J.C., 2012. Linking complex forest fuel structure and fire behaviour at fine scales. Int. J. Wildland Fire 21, 882–893.

Lydersen, J.M., Collins, B.M., Knapp, E.E., Roller, G.B., Stephens, S., 2015. Relating fuel loads to overstorey structure and composition in a fire-excluded Sierra Nevada mixed conifer forest. Int. J. Wildland Fire 24, 484–494.

Mäyrä, J., Keski-Saari, S., Kivinen, S., Tanhuanpää, T., Hurskainen, P., Kullberg, P., Poikolainen, L., Viinikka, A., Tuominen, S., Kumpula, T., 2021. Tree species classification from airborne hyperspectral and LiDAR data using 3D convolutional neural networks. Remote Sens. Environ. 256, 112322.

McCaw, W.L., Neal, J.E., Smith, R.H., 2002. Stand characteristics and fuel accumulation in a sequence of even-aged Karri (Eucalyptus diversicolor) stands in south-west Western Australia. For. Ecol. Manage. 158, 263–271.
McKee, W.H., 1982. Changes in Soil Fertility Following Prescribed Burning On Coastal Plain Pine Sites. US Department of Agriculture, Southeastern Forest Experiment Station, Forest.
Mitchell, R.J., Hiers, J.K., O'Brien, J., Starr, G., 2009. Ecological forestry in the Southeast: understanding the ecology of fuels. J. For. 107, 391–397.
Mitchell, R.J., Kirkman, L.K., Pecot, S.D., Wilson, C.A., Palik, B.J., Boring, L.R., 1999. Patterns and controls of ecosystem function in longleaf pine-wiregrass savannas. I. Aboveground net primary productivity. Can. J. For. Res. 29, 743–751.
Miyaji, K.-.I., Da Silva, W.S., Alvim, P., de, T., 1997. Longevity of leaves of a tropical tree, Theobroma cacao, grown under shading, in relation to position within the canopy and time of emergence. New Phytol. 135, 445–454.
Mugnani, M.P., Robertson, K.M., Miller, D.L., Platt, W.J., 2019. Longleaf pine patch dynamics influence ground-layer vegetation in old-growth pine savanna. Forests 10, 389. https://doi.org/10.3390/f10050389.
Neumann, M., Ukonmaanaho, L., Johnson, J., Benham, S., Vesterdal, L., Novotný, R., Verstraeten, A., Lundin, L., Thimonier, A., Michopoulos, P., Hasenauer, H., 2018. Quantifying carbon and nutrient input from litterfall in European forests using field observations and modeling. Global Biogeochem. Cycles 32, 784–798. https://doi.org/10.1029/2017GB005825.
Noss, R.F., Platt, W.J., Sorrie, B.A., Weakley, A.S., Means, D.B., Costanza, J., Peet, R.K., 2015. How global biodiversity hotspots may go unrecognized: lessons from the North American Coastal Plain. Divers. Distrib. 21, 236–244.
Olson, J.S., 1963. Energy storage and the balance of producers and decomposers in ecological systems. Ecology 44, 322–331.
Ostertag, T.E., Robertson, K.M., 2007. A comparison of native versus old-field vegetation in upland pinelands managed with frequent fire, South Georgia, USA. In: Tall Timbers Fire Ecology Conference Proceedings, pp. 109–120.
Ottmar, R.D., Hudak, A.T., Prichard, S.J., Wright, C.S., Restaino, J.C., Kennedy, M.C., Vihnanek, R.E., 2015. Pre-fire and post-fire surface fuel and cover measurements collected in the south-eastern United States for model evaluation and development – RxCADRE 2008, 2011 and 2012. Int. J. Wildland Fire 25, 10–24. https://doi.org/10.1071/WF15092.
Ottmar, R.D., Restaino, J.C., 2014. RxCADRE 2008, 2011, and 2012: ground fuel measurements from prescribed fires. https://doi.org/10.2737/RDS-2014-0028.
Penne, C., Ahrends, B., Deurer, M., Böttcher, J., 2010. The impact of the canopy structure on the spatial variability in forest floor carbon stocks. Geoderma 158, 282–297. https://doi.org/10.1016/j.geoderma.2010.05.007.
Platt, W.J., Ellair, D.P., Huffman, J.M., Potts, S.E., Beckage, B., 2016. Pyrogenic fuels produced by savanna trees can engineer humid savannas. Ecol. Monogr. 86, 352–372.
Prescott, C.E., 2002. The influence of the forest canopy on nutrient cycling. Tree Physiol. 22, 1193–1200. https://doi.org/10.1093/treephys/22.15-16.1193.
R Core Team, 2021. *R: a language and environment for statistical computing*. R Foundation for Statistical Computing, Vienna. https://www.R-project.org/.
Reid, A.M., Robertson, K.M., 2012. Energy content of common fuels in upland pine savannas of the south-eastern US and their application to fire behaviour modelling. Int. J. Wildland Fire 21, 591–595.
Reid, A.M., Robertson, K.M., Hmielowski, T.L., 2012. Predicting litter and live herb fuel consumption during prescribed fires in native and old-field upland pine communities of the southeastern United States. Can. J. For. Res. 42, 1611–1622.
Reinhardt, E.D., 2003. The Fire and Fuels Extension to the Forest Vegetation Simulator. United States Department of Agriculture, Forest Service, Rocky Mountain.
Robertson, K.M., Hmielowski, T.L., 2014. Effects of fire frequency and season on resprouting of woody plants in southeastern US pine-grassland communities. Oecologia 174, 765–776. https://doi.org/10.1007/s00442-013-2823-4.
Robertson, K.M., Hsieh, Y.P., Bugna, G.C., 2014. Fire environment effects on particulate matter emission factors in southeastern US pine-grasslands. Atmos. Environ. 99, 104–111.
Robertson, K.M., Platt, W.J., Faires, C.E., 2019. Patchy fires promote regeneration of longleaf pine (Pinus palustris Mill.) in pine savannas. Forests 10, 367.
Rocha, K.D., Silva, C.A., Cosenza, D.N., Mohan, M., Klauberg, C., Schlickmann, M.B., Xia, J., Leite, R.V., Almeida, D.R.A.de, Atkins, J.W., Cardil, A., Rowell, E., Parsons, R., Sánchez-López, N., Prichard, S.J., Hudak, A.T., 2023. Crown-level structure and fuel load characterization from airborne and terrestrial laser scanning in a longleaf pine (Pinus palustris Mill.) forest ecosystem. Remote Sens. (Basel) 15, 1002. https://doi.org/10.3390/rs15041002.
Rother, M.T., Huffman, J.M., Guiterman, C.H., Robertson, K.M., Jones, N., 2020. A history of recurrent, low-severity fire without fire exclusion in southeastern pine savannas, USA. For. Ecol. Manag. 475, 118406.
Roussel, J.-.R., Auty, D., Coops, N.C., Tompalski, P., Goodbody, T.R., Meador, A.S., Bourdon, J.-.F., de Boissieu, F., Achim, A., 2020. lidR: an R package for analysis of Airborne Laser Scanning (ALS) data. Remote Sens. Environ. 251, 112061.
Schoettle, A.W., Fahey, T.J., Shoettle, A.W., 1994. Foliage and fine root longevity of pines. Ecol. Bull. 136–153.
Semenova-Nelsen, T.A., Platt, W.J., Patterson, T.R., Huffman, J., Sikes, B.A., 2019. Frequent fire reorganizes fungal communities and slows decomposition across a heterogeneous pine savanna landscape. New Phytol. 224, 916–927. https://doi.org/10.1111/nph.16096.
Senay, G., Kagone, S., 2019. Daily SSEBop evapotranspiration data from 2000 to 2018. https://doi.org/10.5066/P9L2YMV.
Senay, G.B., Bohms, S., Singh, R.K., Gowda, P.H., Velpuri, N.M., Alemu, H., Verdin, J.P., 2013. Operational evapotranspiration mapping using remote sensing and weather datasets: a new parameterization for the SSEB approach. JAWRA J. Am. Water Resour. Assoc. 49, 577–591. https://doi.org/10.1111/jawr.12057.
Shi, Y., Skidmore, A.K., Wang, T., Holzwarth, S., Heiden, U., Pinnel, N., Zhu, X., Heurich, M., 2018. Tree species classification using plant functional traits from LiDAR and hyperspectral data. Int. J. Appl. Earth Observ. Geoinform. 73, 207–219.
Silva, C.A., Hudak, A.T., Vierling, L.A., Loudermilk, E.L., O'Brien, J.J., Hiers, J.K., Jack, S.B., Gonzalez-Benecke, C., Lee, H., Falkowski, M.J., 2016. Imputation of individual longleaf pine (Pinus palustris Mill.) tree attributes from field and LiDAR data. Can. J. Remote Sens. 42, 554–573.
Soil Survey Staff, 2021. Web soil survey. National Resources Conservation Service, USDA.
Silva, C.A., Klauberg, C., Hudak, A.T., Vierling, L.A., Jaafar, W.S.W.M., Mohan, M., Garcia, M., Ferraz, A., Cardil, A., Saatchi, S., 2017. Predicting stem total and assortment volumes in an industrial Pinus taeda L. forest plantation using airborne laser scanning data and random forest. Forests 8, 254.
Stevens-Rumann, C.S., Hudak, A.T., Morgan, P., Arnold, A., Strand, E.K., 2020. Fuel dynamics following wildfire in US Northern Rockies forests. Front. For. Glob. Change 3.
Thaxton, J.M., Platt, W.J., 2006. Small-scale fuel variation alters fire intensity and shrub abundance in a pine savanna. Ecology 87, 1331–1337.
Thomas, H., Stoddart, J.L., 1980. Leaf senescence. Annu. Rev. Plant Physiol. 31, 83–111.
Southeast (SE) FireMap, 2021. URL https://www.landscapepartnership.org/key-issues/wildland-fire/fire-mapping/regional-fire-mapping/se-firemap/se-firemap-collection (accessed 3.15.22).
Thornton, M.M., Shrestha, R., Wei, Y., Thornton, P.E., Kao, S.-.C., Wilson, B.E., 2020. Daymet: annual climate summaries on a 1-km grid for North America, version 4. ORNL DAAC. https://doi.org/10.3334/ORNLDAAC/1852.
Tupek, B., Mäkipää, R., Heikkinen, J., Peltoniemi, M., Ukonmaanaho, L., Hokkanen, T., Nöjd, P., Nevalainen, S., Lindgren, M., Lehtonen, A., 2015. Foliar turnover rates in Finland-comparing estimates from needle-cohort and litterfall-biomass methods.
USDA-FIA, 2021. Forest type groups of the continental United States, https://di-usfs.img.arcgis.com/arcgis/rest/services/CONUS_forest_type_group_2018_masked_202105122120120/ImageServer (last accessed 2/3/2023).
USDA-USFS, 2022. Forest Atlas of the United States. https://doi.org/10.2737/FS-1172.
Walker, J., Peet, R.K., 1984. Composition and species diversity of pine-wiregrass savannas of the Green Swamp, North Carolina. Vegetatio 55, 163–179.
Wan Mohd Jaafar, W.S., Woodhouse, I.H., Silva, C.A., Omar, H., Abdul Maulud, K.N., Hudak, A.T., Klauberg, C., Cardil, A., Mohan, M., 2018. Improving individual tree crown delineation and attributes estimation of tropical forests using airborne LiDAR data. Forests 9, 759.
White, M.A., Thornton, P.E., Running, S.W., Nemani, R.R., 2000. Parameterization and sensitivity analysis of the BIOME–BGC terrestrial ecosystem model: net primary production controls. Earth Interact. 4, 1–85.
Wiegert, R.G., Monk, C.D., 1972. Litter production and energy accumulation in three plantations of longleaf pine (Pinus palustris Mill). Ecology 53, 949–953.
Wilson, B.T., Knight, J.F., McRoberts, R.E., 2018. Harmonic regression of Landsat time series for modeling attributes from national forest inventory data. ISPRS J. Photogramm. Remote Sens. 137, 29–46. https://doi.org/10.1016/j.isprsjprs.2018.01.006, 137, 29–46.
Wilson, B.T., Lister, A.J., Riemann, R.I., 2012. A nearest-neighbor imputation approach to mapping tree species over large areas using forest inventory plots and moderate resolution raster data. For. Ecol. Manage. 271, 182–198. https://doi.org/10.1016/j.foreco.2012.02.002, 271, 182–198.
Wilson, B.T., Woodall, C.W., Griffith, D.M., 2013. Imputing forest carbon stock estimates from inventory plots to a nationally continuous coverage. Carbon Balance Manag. 8, 1–15. https://doi.org/10.1186/1750-0680-8-1.
Yarie, J., 2000. Boreal forest ecosystem dynamics. I. A new spatial model. Can. J. For. Res. 30, 998–1009. https://doi.org/10.1139/x99-168.
Zazali, H.H., Towers, I.N., Sharples, J.J., 2020. A critical review of fuel accumulation models used in Australian fire management. Int. J. Wildland Fire.
Zhao, D., Bullock, B.P., Montes, C.R., Wang, M., Greene, D., Sutter, L., 2019a. Loblolly pine outperforms slash pine in the southeastern United States–a long-term experimental comparison study. For. Ecol. Manage. 450, 117532.
Zhao, D., Kane, M., Markewitz, D., Teskey, R., Clutter, M., 2015. Additive tree biomass equations for midrotation loblolly pine plantations. For. Sci. 61, 613–623.
Zhao, D., Kane, M., Teskey, R., Markewitz, D., 2016. Modeling aboveground biomass components and volume-to-weight conversion ratios for loblolly pine trees. For. Sci. 62, 463–473.
Zhao, D., Westfall, J., Coulston, J.W., Lynch, T.B., Bullock, B.P., Montes, C.R., 2019b. Additive biomass equations for slash pine trees: comparing three modeling approaches. Can. J. For. Res. 49, 27–40. https://doi.org/10.1139/cjfr-2018-0246.